

This is the final peer-reviewed accepted manuscript of:

Roldán-Peña JM, Alexandre-Ramos D, López Ó, Maya I, Lagunes I, Padrón JM, Peña-Altamira LE, Bartolini M, Monti B, Bolognesi ML, Fernández-Bolaños JG. *New tacrine dimers with antioxidant linkers as dual drugs: Anti-Alzheimer's and antiproliferative agents*. Eur J Med Chem. 2017 Sep 29; 138:761-773.

The final published version is available online at:
<https://doi.org/10.1016/j.ejmech.2017.06.048>

Rights / License:

The terms and conditions for the reuse of this version of the manuscript are specified in the publishing policy. For all terms of use and more information see the publisher's website.

This item was downloaded from IRIS Università di Bologna (<https://cris.unibo.it/>)

When citing, please refer to the published version.



**New tacrine-phenolics as
multi target anti-Alzheimer derivatives**

**Up to subnanomolar
inhibitors of BuChE**

**Inhibition of
Aβ₄₂ self-aggregation**

**Neuroprotective
effects**

**Lack of
neurotoxicity**

**Low
hepatotoxicity**

Tacrine-phenols heterodimers as multitarget-directed ligands against Alzheimer's disease: selective subnanomolar BuChE inhibitors

Jesús M. Roldán-Peña,^a Valle Romero-Real,^a Javier Hicke,^a Inés Maya,^a Antonio Franconetti,^b Irene Lagunes,^c José M. Padrón,^c Sabrina Petralla,^d Eleonora Poeta,^d Marina Naldi,^d Manuela Bartolini,^d Barbara Monti,^d Maria L. Bolognesi,^d Óscar López^{a,*} José G. Fernández-Bolaños^{a,*}

^aDepartamento de Química Orgánica, Facultad de Química, Universidad de Sevilla, Apartado 1203, E-41071 Sevilla, Spain. Email: bolanos@us.es, osc-lopez@us.es

^b Department de Química, Universitat Autònoma de Barcelona, 08193 Cerdanyola del Vallè, Spain

^cBioLab, Instituto Universitario de Bio-Orgánica "Antonio González" (IUBO-AG), Centro de Investigaciones Biomédicas de Canarias (CIBICAN), Universidad de La Laguna, Apartado 456, E-38071 La Laguna, Spain

^dDepartment of Pharmacy and Biotechnology, Alma Mater Studiorum University of Bologna, via Belmeloro 6, 40126 Bologna, Italy

Highlights

- A series of tacrine-phenolic hybrids have been accessed as MTDL's for Alzheimer's disease
- Nature/length of the linker (imine, amine, ether) and type of aryl substituents have been modified
- Strong and selective BuChE inhibitors have been obtained (low nanomolar-subnanomolar)
- Good A β inhibition and neuroprotection profiles were observed
- Low neurotoxicity and hepatotoxicity for the lead compound were observed

Tacrine-polyphenols heterodimers as multitarget-directed ligands against Alzheimer's disease: selective subnanomolar BuChE inhibitors

Jesús M. Roldán-Peña,^a Valle Romero-Real,^a Javier Hicke,^a Inés Maya,^a Antonio Franconetti,^b Irene Lagunes,^c José M. Padrón,^c Sabrina Petralla,^d Eleonora Poeta,^d Marina Naldi,^d Manuela Bartolini,^d Barbara Monti,^d Maria L. Bolognesi,^d Óscar López^{a,*} José G. Fernández-Bolaños^{a,*}

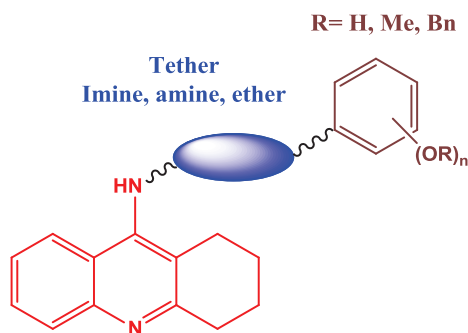
^aDepartamento de Química Orgánica, Facultad de Química, Universidad de Sevilla, Apartado 1203, E-41071 Sevilla, Spain. Email: bolanos@us.es, osc-lopez@us.es

^b Department de Química, Universitat Autònoma de Barcelona, 08193 Cerdanyola del Vallè, Spain

^c BioLab, Instituto Universitario de Bio-Orgánica "Antonio González" (IUBO-AG), Centro de Investigaciones Biomédicas de Canarias (CIBICAN), Universidad de La Laguna, Apartado 456, E-38071 La Laguna, Spain

^d Department of Pharmacy and Biotechnology, Alma Mater Studiorum University of Bologna, via Belmeloro 6, 40126 Bologna, Italy

Graphical abstract



New tacrine-phenolics as multi target anti-Alzheimer derivatives

Up to subnanomolar inhibitors of BuChE Inhibition of AB₄₂ self-aggregation Neuroprotective effects Lack of neurotoxicity Low hepatotoxicity

Highlights

- A series of tacrine-phenolic hybrids have been accessed as MTDL's for Alzheimer's disease
- Nature/length of the linker (imine, amine, ether) and type of aryl substituents have been modified
- Strong and selective BuChE inhibitors have been obtained (low nanomolar-subnanomolar)
- Good Aβ inhibition and neuroprotection profiles were observed
- Low neurotoxicity and hepatotoxicity for the lead compound were observed

Abstract

Concerned by the devastating effects of Alzheimer's disease, and the lack of effective drugs, we have carried out the design of a series of tacrine-phenolic heterodimers in order to tackle the multifactorial nature of the disease.

Hybridization of both pharmacophores involved the modification of the nature (imino, amino, ether) and the length of the tether, together with the type (hydroxy, methoxy, benzyloxy), number and position of the substituents on the aromatic residue. Title compounds were found to be strong and selective inhibitors of human BuChE (from low nanomolar to subnanomolar range), an enzyme that becomes crucial in the more advanced stages of the disease.

The lead compound, bearing an ether-type tether, had an IC_{50} value of 0.52 nM against human BuChE, and a selectivity index of 323, with an 85-fold increase of activity compared to parent tacrine; key interactions were analysed using molecular modelling. Moreover, it also inhibited the self-aggregation of $A\beta_{42}$, lacking neurotoxicity up to 5 μ M concentration, and showed neuroprotective activity in primary rat neurons in a serum and K^+ deprivation model, widely employed for reproducing neuronal injury and senescence. Moreover, low hepatotoxicity effects and complete stability under physiological conditions were found for that compound.

So, overall, our lead compound can be considered as a promising multitarget-directed ligand against Alzheimer's disease, and a good candidate for developing new drugs.

Keywords: Alzheimer's disease, tacrine, heterodimers, multitarget, BuChE

1. Introduction

Alzheimer's disease was firstly reported as a rare disorder by the German psychiatrist Alois Alzheimer in 1906 [1]. Such uncommon neuropsychiatric disorder has become nowadays the main form of senile dementia; roughly 70% of cases can be attributed to Alzheimer's disease [2]. According to the *World Alzheimer Report 2018* [3], 50-million cases have already been reached, and an exponential rise is expected to afford 152-million cases in 2050; this means a new reported case each 3.2 s [4].

Alzheimer's remains as one of the most current devastating diseases; although the most recognizable symptom is memory loss, many others, like depression, cognitive impairment, behavioural changes, or psychosis, among others are also associated with the progression of this pathology [5]. Alzheimer's disease also involves a severe economic burden [3] to the World Health Systems, and to the families. More frustrating, no drug is available for the cure of Alzheimer's; the only four marketed drugs only allow palliative and temporal improvement of the cognitive functionality for the early to moderate stages.

From a pathophysiological point of view, Alzheimer's disease is an extraordinary complex pathology, with a multifactorial etiology, lacking a single triggering cause. Accordingly, this situation hinders the development of a successful drug [6,7]. From a microscopic point of view, two hallmarks have been reported: cortical amyloidogenesis, which leads to the extracellular deposits of toxic β -amyloid, mainly $A\beta_{42}$ [8], and the intraneuronal accumulation of neurofibrillary tangles, as a result from the hyperphosphorylation of tau protein [9]. Some other events that also contribute to neurodegeneration are mitochondrial dysfunction, oxidative stress, pro-inflammatory responses, or the alteration of the homeostasis of biometals [9–11]. Moreover, abnormally low levels of the neurotransmitter acetylcholine, which is responsible for the cognitive functionality, are also found in the brain of Alzheimer's patients [12].

Due to the extremely complex nature of the disease, it is currently claimed [13,14] that a shift is required for the successful treatment of Alzheimer's disease, from the classical *one-target-one-drug* philosophy to multitarget-directed ligands (MTDLs) approach [15], which tackle several therapeutic targets simultaneously.

In this context, we envisioned the possibility of preparing tacrine heterodimers as multitarget ligands against Alzheimer's disease; tacrine, a cholinesterase inhibitor, was the first Alzheimer's drug approved by FDA (1993), but it was withdrawn shortly after because of its **hepatotoxicity**, probably due to its pro-oxidant character [16]. In spite of that, tacrine has been largely investigated as starting scaffold for the synthesis of MTDLs for Alzheimer therapy [17].

Amalgamating tacrine structure in new hybrid molecules should improve its biological profile and overcome undesirable side effects. In particular, we propose the hybridization of tacrine (ensuring cholinesterase inhibition), with a phenolic residue, which might provide access to other relevant therapeutic targets, like the modification of the neuronal redox status, or the accumulation of toxic A β peptides in brain.

In order to get some insight into the structural requirements for obtaining the lead-compounds, we planned the modification of the nature of the tether linking both pharmacophores, as well as the type and position of substituents on the aromatic scaffold (Figure 1). The inhibition of cholinesterases and deposition of amyloid plaque, **neuroprotection, hepatotoxicity, and neurotoxicity** will be evaluated in order to get a more defined pharmacological profile of the new compounds.

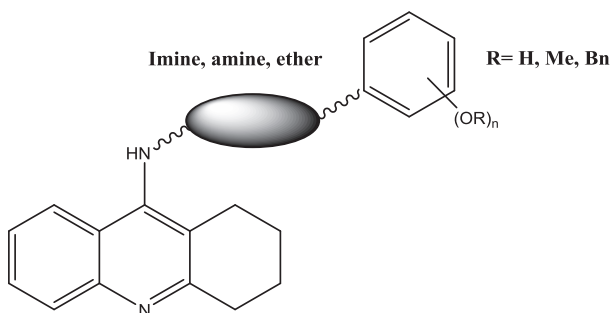


Figure 1. General structure for the tacrine-polyphenolic heterodimers prepared herein

2. Results and discussion

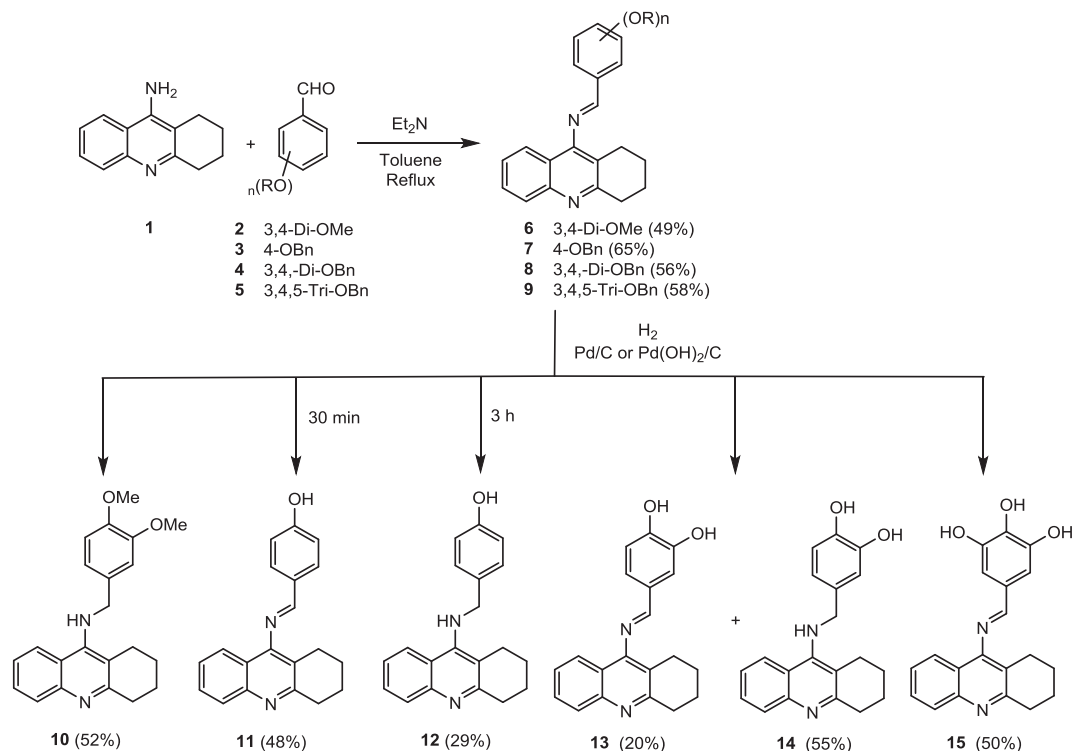
2.1. Chemistry

In a first approach, the condensation of parent tacrine **1** with *O*-protected phenolic aldehydes **2–5** was attempted (Scheme 1) to furnish the corresponding imines **6–9**, featured with restricted rotation. Initially, a classical acid-catalysed procedure was assayed, but the yields were sensibly lower than using **basic** catalysis (Et₂NH); resonances at 8.10–8.25 (¹H-NMR, azomethine proton) and roughly 160 ppm (¹³C-

NMR, N=CH) confirmed the proposed structures. Moreover, due to the extended conjugation, such imines were endowed with high stability, even in solution.

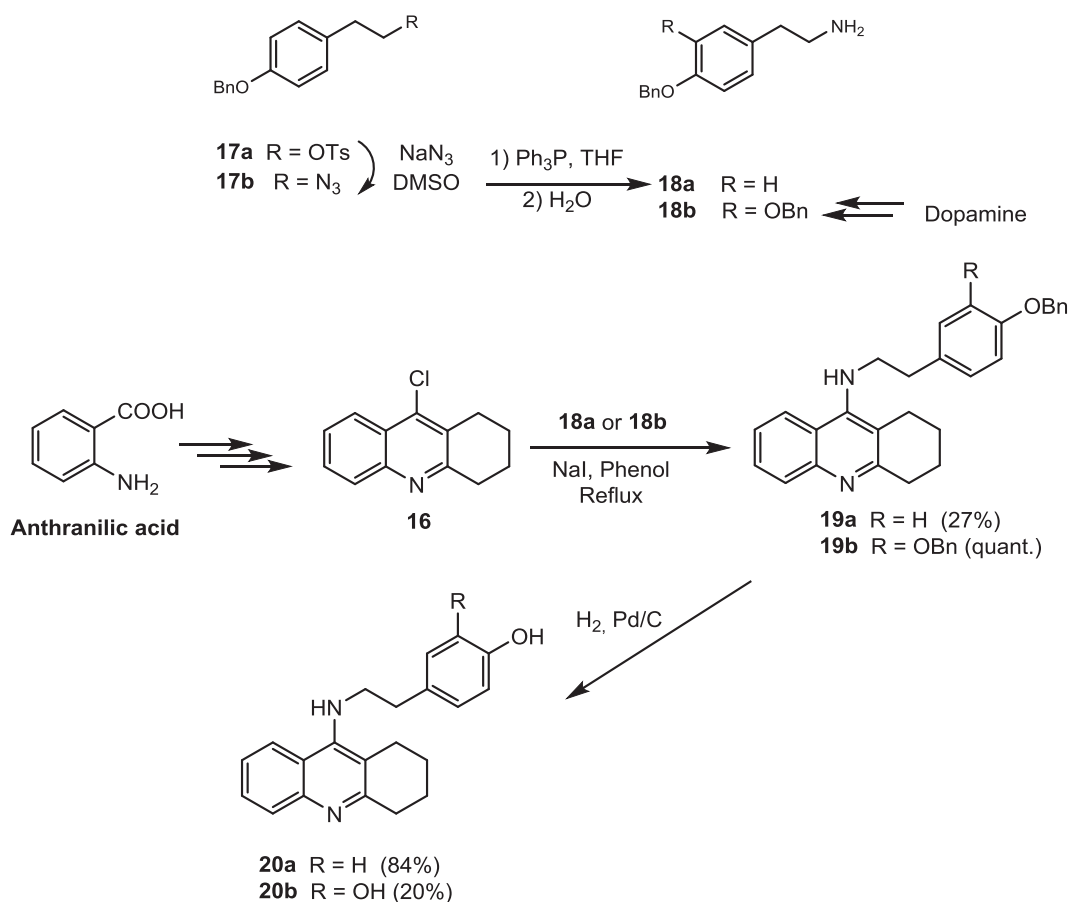
Next, the hydrogenolysis of the Schiff base was accomplished, in order to provide the compounds with conformational flexibility around the nitrogen atom (benzyl amines **10**, **12**, **14**); Pd/C, Pd(OH)₂/C and Raney Ni were evaluated as catalysts, **the two former being the optimal ones**.

The low reactivity of the imine functionality was also demonstrated in this reaction; thus, hydrogenolysis of dimethoxy derivative **6** allowed the isolation of **10** [18] in a 52% yield, and the recovery of 48% of the starting material after a 6-h reaction (Scheme 1). Moreover, when reduction of the *p*-benzyl substituted **7** was accomplished in a short reaction time (30 min), only *p*-hydroxy-imine **11** was isolated (48% yield); more prolonged treatments (3 h) afforded the isolation of **12** (29% yield). In the case of the dibenzylated imine **8**, a mixture of catechol-containing imine **13** (20%), together with benzylamine **14** (55%) was obtained. Nevertheless, for tribenzylated imine **9**, only the removal of benzyl protecting groups was achieved (**15**, 50%); attempts to reduce the imine functionality led to unexpected extensive decomposition.



Scheme 1. **Synthesis of tacrine-phenolic hybrids with an imine or amine tether**

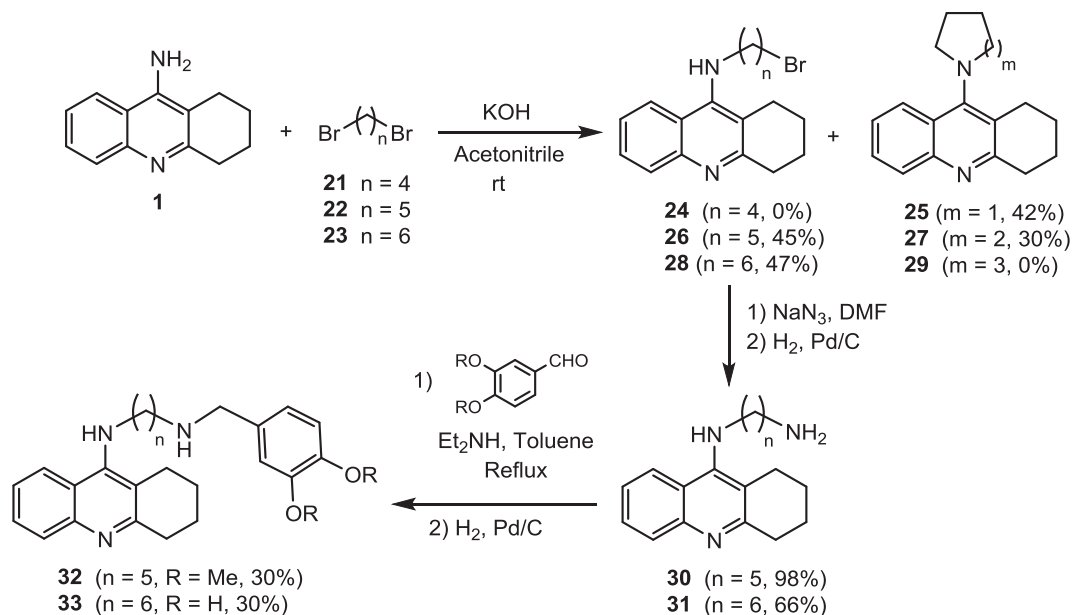
In order to increase the length of the tether connecting tacrine and the polyphenolic scaffolds, we also designed the preparation of phenethylamines **20a** and **20b** (Scheme 2); such compounds can be considered as hybrid structures of tacrine and tryramine/dopamine. Moreover, the influence of the number of phenolic hydroxyl groups will also be analysed for the bioactivities of such compounds. For that purpose, 9-chloro-1,2,3,4-tetrahydroacridine **16**, obtained by POCl₃-promoted condensation between anthranilic acid and cyclohexanone, was proposed as a valuable intermediate. Next, nucleophilic attack exerted by *O*-protected derivatives **18a** and **18b** in refluxing phenol, furnished derivatives **19a,b** from modest to quantitative yields, which in turn were deprotected to give the hitherto unknown heterodimers **20a,b**.



Scheme 2. Preparation of tacrine-tyramine/dopamine hybrids

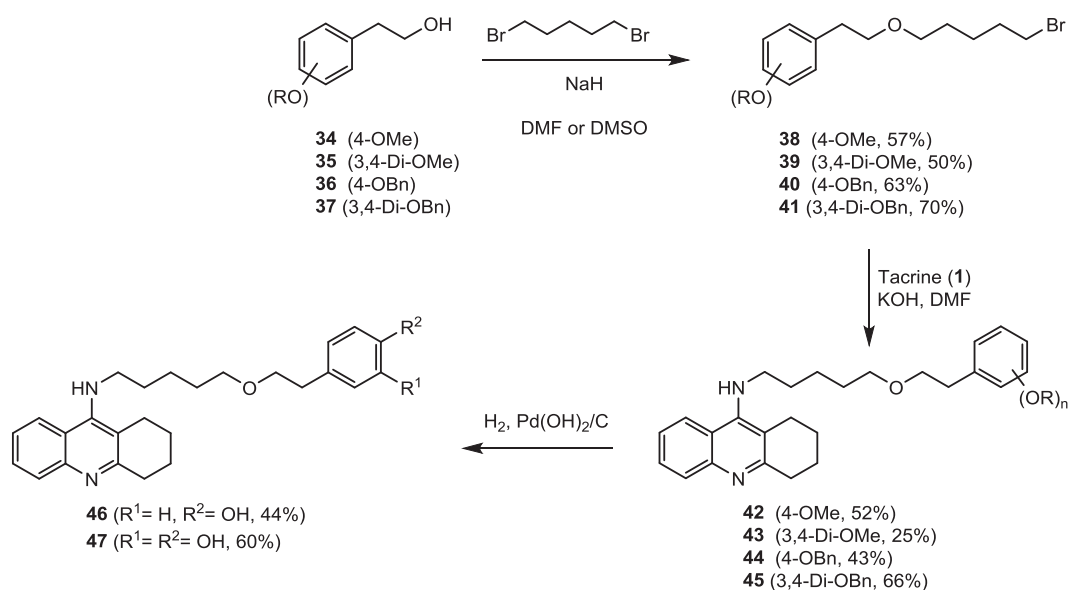
In order to increase further the length of the tether, and to introduce a second nitrogen atom that might be involved in non-covalent interactions with cholinesterases, the synthetic pathway depicted in Scheme 3 was followed. The first step involves the monoalkylation of parent tacrine with α,ω -dibromoalkanes **21–23** under basic conditions. Nevertheless, for 1,4-dibromobutane, no monoalkylated product was detected, and 9-pyrrolidine derivative **25** was obtained as the only product through a second intramolecular nucleophilic substitution (42%). Use of 1,5-dibromopentane afforded the isolation of monoalkylated derivative **26** as the major compound (45%), together with the corresponding 9-piperidinyl derivative **27** (30%); only when 1,6-dibromohexane was employed, the corresponding monoalkylated product (**28**, 47%) was obtained as the only product.

Next, nucleophilic substitution of the terminal bromine atom with NaN_3 , followed by reduction of the azido group furnished ω -amino derivatives **30, 31** (Scheme 3). Finally, base-catalysed condensation of such compounds with *O*-protected benzaldehydes, followed by catalytic hydrogenation of the benzyl groups afforded dimethoxy and dihydroxylated derivatives **32** and **33**, respectively (Scheme 3).



Scheme 3. Synthesis of tacrine-phenolic hybrids with an aminoalkyl linker

Finally, ether isosters of **32** and **33** were prepared following the synthetic pathway showed in Scheme 4; isosteric replacement of the nitrogen atom with oxygen might confer different binding properties within the enzyme active site, thus modulating the inhibitory properties. Alkylation of substituted 2-phenyl ethanol derivatives **34–37** with 1,6-dibromopentane to give the monobromo derivatives **38–41**, followed by nucleophilic displacement of the terminal bromine atom with tacrine furnished derivatives **42–45** from moderate to good yields (25–66%); deprotection of the benzyl functionalities of **44–45** gave access to mono- and dihydroxylated derivatives **46, 47**.



Scheme 4. Preparation of tacrine-polyphenols hybrids with an alkyl-ether linker

2.2. Biological assessment

2.2.1. Cholinesterases and A β -self aggregation inhibition

A common feature affecting patients suffering from Alzheimer's disease is the low level of neurotransmitter acetylcholine, which in turn provokes a decline of the cognitive function, including memory and thinking skills [19]. Some years ago it was established that inhibitors of cholinesterases (acetylcholinesterase-AChE and butyrylcholinesterase-BuChE) can be useful in restoring the levels of acetylcholine, and

are therefore of high therapeutic interest; this is known as the *cholinergic hypothesis* [20].

It has been reported that AChE, which accounts for 90% of the termination of the signal in the cholinergic neurons in healthy brains, undergoes a significant reduction within the progression of the disease; whereas BuChE, whose biological roles have not been completely elucidated, either remains unchanged, or increases [21], particularly in the brain regions associated with cognition and behaviour [22]. BuChE has also been found to associate with amyloid plaques and neurofibrillary tangles both in human tissues, and in mouse models, and is probably involved in their maturation to initiate neurodegeneration [23]. Moreover, administration of selective BuChE inhibitors is not only proposed to be more beneficial for advanced stages of Alzheimer's disease, but could also avoid the onset of the cholinergic side-effects commonly associated with the administration of AChE inhibitors [24].

Compounds prepared herein were initially screened *in vitro* against AChE (*Electrophorus electricus*) and BuChE (equine serum), which are currently considered as good model enzymes. Those exhibiting strong inhibitory properties against the model enzymes were selected for further evaluation against the human ones. For that purpose, the Ellman's colorimetric assay [25] was used, in which acetyl- and butyryl-thiocholine iodides are used as analogues of the natural substrate; reaction takes place in the presence of 5,5'-dithiobis(2-nitrobenzoic acid) (DTNB) as a chromogen reagent, and activity is measured in an indirect way by monitoring the absorbance increase at 405 nm associated to the *in situ* generation of 5-thio-2-nitrobenzoate anion (pH 8.0).

Valuable structure-activity relationships (SARs) can be extracted from data listed in Table 1; tacrine and galantamine are included as reference drugs.

Regarding AChE and the first set of compounds (imines and amines **6–15**), the presence of one or two benzyl groups (compounds **7**, **8**) provoke an impairment of activity, leading to only a moderate inhibitory activity ($K_i = 20\text{--}39\ \mu\text{M}$). Interestingly, replacement of two benzyl groups with methoxy moieties (compound **6**) furnished a roughly 10-fold increase of activity, with inhibition constants within the low micromolar range. A similar effect was observed upon removal of the benzyl group to achieve the free phenolic imines **11** and **13**. However, and unexpectedly, incorporation

of three benzyl groups (compound **9**) allowed virtually the same degree of inhibitory activity as found for counterpart **6**.

Moreover, in most cases, conformationally-flexible and more basic amines were found to exhibit higher inhibitory properties than parent imines, shifting from activities within the low micromolar range to the submicromolar range (**11** vs. **12**, **13** vs. **14**). Two effects might be responsible for such results; on the one hand, the increased conformational flexibility of the benzylamino functionality compared to the more rigid imino group might enable the establishment of favourable interactions within the catalytic site of the enzyme. On the other hand, the higher basicity of the amino group compared to the imine would favour the formation of the ammonium cation, which better resembles the natural substrate of the enzyme. We have recently found that conversion of tacrine into amides strongly diminished the inhibitory action on AChE [26].

Furthermore, regarding imines, an increase in the number of free hydroxyl groups was proved to significantly improve inhibitory properties against AChE; thus, comparison between derivatives **11**, **13** and **15** (mono-, di- and trihydroxylated imines) shows that trihydroxylated derivative **15** is endowed with an up to 10-fold higher activity (Table 1) compared to the other two partners of the series (K_i 's= 0.40 and 0.17 μ M). The effect is less pronounced when considering more active amine-counterparts; thus, dimethoxy derivative **10** [18] is already a strong AChE inhibitor, and the activity is mildly improved (up to 3-fold) by inserting one (**12**) or two hydroxyl groups (**14**). Elongation of the tether in the polyhydroxylated amines (e.g. **10** vs. **32** [27]) also slightly improved the activity. However, comparison of tacrine/tyramine or tacrine/dopamine hybrids (compounds **20a** and **20b**, respectively), showed a reversed behaviour for AChE, as depicted in Table 1.

Finally, most of the tested compounds turned out to be more potent inhibitors than galantamine, which is currently in clinical use for the treatment of mild to moderate Alzheimer's cases.

Free polyhydroxylated compounds are not only endowed with potent inhibitory properties against AChE, but also with antioxidant capacity, capable of altering the redox status of the cells in Alzheimer's patients. Moreover, it has recently been reported that the use of bulky aromatic fragments on C-9 can avoid the interaction of the

tetrahydroacridine core with the heme-iron center of cytochrome P450 enzyme, thus, reducing the inherent hepatotoxicity of tacrine [28].

Interestingly, all the tacrine-polyphenolic hybrids prepared herein showed remarkable selectivity towards BuChE, which exerts a more prominent role at later stages of the disease. The volume of the active site gorge is considerably higher (roughly 200 Å³) than the one found in AChE [29], so BuChE can accommodate bulkier inhibitors, and this may constitute the basis for the selectivity of these derivatives.

Inhibition of BuChE spanned over a quite wide range of potencies, ranging from low micromolar to low nanomolar values (Table 1). The most potent compounds turned out to be the ones bearing an ether-type linker, with more than 4000-fold higher activity in comparison with galantamine.

Some of the most remarkable examples within each family (polyhydroxylated imines, amines and ether-types) were selected for further studies as potential anti-Alzheimer's agents. Firstly, they were evaluated as inhibitors of the human enzymes (hAChE and hBuChE). The calculated IC₅₀ values are listed in Table 2.

Regarding the influence of the number of hydroxyl groups for the amino-type tether, comparison of dihydroxylated derivative **33** and its mono-hydroxylated counterpart, the latter already reported by Luo *et al.* [27] showed virtually no change in the AChE inhibition (Table 2; 29.0 vs. 25.6 nM, respectively), and a moderate increase in selectivity towards BuChE (1.3 vs. 3.4, respectively).

Clearly, imines and amines behaved as much weaker inhibitors than ether-containing derivatives; compounds **42**, **44**, **46** were strong hBuChE inhibitors with activities in the low nanomolar range. In particular, the dimethoxy derivative **43** and dibenzyloxy derivative **45** were found to be extremely potent inhibitors of title enzyme, within the subnanomolar range; this represents a roughly 85-fold increase compared to the parent tacrine, used herein as a reference drug. Accordingly, the key structural motifs for achieving the highest inhibitory potency are the presence of the tacrine core, an ether-type tether, and a dialkoxylated phenyl residue. Dialkoxylated derivatives were found to be much stronger inhibitors of hBuChE than their mono-substituted counterparts (**42** vs. **43**, **44** vs. **45**).

All the ether-containing derivatives were tested as potential *in vitro* inhibitors for the Aβ self-aggregation (1:1 inhibitor/Aβ ratio), another relevant hallmark in

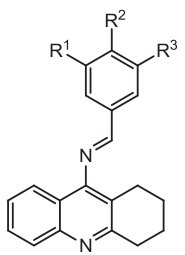
Alzheimer's disease (data shown in Table 2); for that purpose, the thioflavin-T fluorescence assay was used [30]. All tested derivatives exerted a significant inhibition of amyloid self-aggregation with inhibitory potencies in a relatively close range (from 54.4 to 74.3%). Despite the limited number of tested compounds, some considerations could be drawn. In particular, the type of substituent at the aromatic ring seems to influence activity and the following trend can be observed: OBn>OMe>OH. On the other hand, the mono or disubstitution pattern does not seem to influence the inhibitory activity.

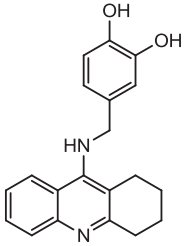
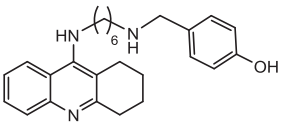
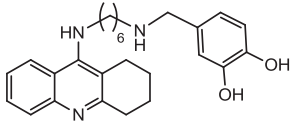
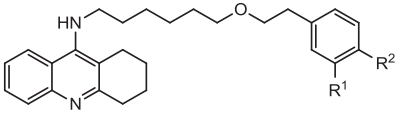
Thus the mono- and di-substituted benzyloxy derivatives **44** and **45** were the most potent derivatives, showing inhibitory potencies similar to that of the known multipotent compound bis(7)tacrine, a tacrine homodimer, which is one of the most prominent tacrine-based cholinesterase inhibitors reported so far [31]. Inhibitory activity of compound **47** could not be determined because of a significant interference in the assay conditions (quenching of the thioflavin T fluorescence signal).

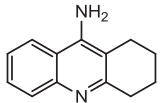
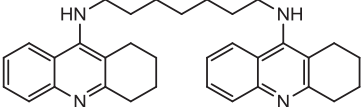
Table 1. Inhibitory properties of tacrine-polyphenols ($K_i \pm SD$)							
Compound	Series	AChE (<i>electric eel</i>)		Type of inhibitor	BuChE (equine serum)		Type of inhibitor
		K_{ia} (μM)	K_{ib} (μM)		K_{ia} (nM)	K_{ib} (nM)	
6	Imine	2.5 ± 0.6	1.9 ± 0.4	Mixed	271 ± 36	35 ± 8	Mixed
7		39 ± 10	23 ± 6		2925 ± 1183	643 ± 327	
8		24 ± 4	20 ± 1		637 ± 79	173 ± 42	
9		2.3 ± 0.8	3.0 ± 0.8		704 ± 82	192 ± 74	
10	Amine (1C)	0.64 ± 0.08	0.21 ± 0.06		31 ± 6	6.4 ± 1.3	
11	Imine	3.0 ± 0.6	1.8 ± 0.1		---	17 ± 5	Uncompetitive
12	Amine (1C)	0.37 ± 0.04	0.081 ± 0.013		12 ± 2	3.2 ± 0.5	Mixed
13	Imine	2.1 ± 0.3	0.82 ± 0.27		11 ± 4	1.9 ± 0.8	
14	Amine (1C)	0.19 ± 0.06	0.19 ± 0.06		Non-competitive	25 ± 6	
15	Imine	0.40 ± 0.19	0.17 ± 0.04		Mixed	51 ± 17	5.8 ± 1.5

19	Amine (2C)	1.6 ± 0.5	0.61 ± 0.15	Mixed	22 ± 7	1.1 ± 0.6	
20a		0.11 ± 0.01	0.032 ± 0.005	Mixed	184 ± 46 (Uncompetitive)		
20b		0.87 ± 0.43	0.59 ± 0.38	Mixed	128 ± 20	28 ± 9	
25	Cyclic amine	3.2 ± 0.8	---	Competitive	1202 ± 130	304 ± 81	
27		1.8 ± 1.2	2.5 ± 1.5	Mixed	1898 ± 590	275 ± 105	
32	Amine	0.16 ± 0.09	0.12 ± 0.03		30 ± 14	9.9 ± 3.7	
33	(5- and 6C)	0.12 ± 0.05	0.058 ± 0.015		7.9 ± 1.0	1.7 ± 0.4	
42	Ether	0.075 ± 0.028	0.075 ± 0.028	Non- competitive	29 ± 5	2.9 ± 1.1	
43		0.17 ± 0.02	0.055 ± 0.016	Mixed	7.0 ± 0.4	1.9 ± 0.8	
44		0.11 ± 0.02	0.11 ± 0.02	Non- competitive	1.9 ± 0.9	1.5 ± 0.9	
45		0.34 ± 0.05	0.13 ± 0.03	Mixed	4.6 ± 0.6	2.7 ± 0.9	
46		0.14 ± 0.02	0.10 ± 0.06		---	4.5 ± 1.5	Uncompetitive
47		0.21 ± 0.02	0.077 ± 0.016		43 ± 7	9.0 ± 2.2	Mixed

Tacrine		0.023 ± 0.010	---	Competitive	17 ± 3	---	Competitive
Galantamine		3.0 ± 0.9	---		7700 ± 1700	---	

Table 2. Anti-Alzheimer's properties of selected compounds					
Compound		hAChE (IC₅₀, nM)	hBuChE (IC₅₀, nM)	Selectivity index (SI)	%Inhibition Aβ₄₂ self-aggregation (at 50 μM)
11 (R ¹ = R ³ = H, R ² = OH)		1475 ± 311	194±15	7.6	---
13 (R ¹ = H, R ² = R ³ = OH)		609 ± 26	41.5 ± 4.06	14.8	---
15 (R ¹ = R ² = R ³ = OH)		1040 ± 40	120±49	8.7	---

14		100 ± 13	$74,8 \pm 3,4$	1.3	---
---		25.6 ± 0.9 Ref [27]	7.50 ± 0.02 Ref [27]	3.4	---
33		$29,0 \pm 1,3$	$22,9 \pm 1,2$	1.3	---
42 (R ¹ = H, R ² = OMe)		216 ± 45	2.92 ± 0.26	74.5	$63,5 \pm 1,0$
43 (R ¹ = R ² = OMe)		168 ± 37	0.515 ± 0.050	323.1	$63,8 \pm 4,8$
44 (R ¹ = H, R ² =		454 ± 69	6.95 ± 0.21	65.8	$70,0 \pm 4,8$

OBn)					
45 (R ¹ = R ² = OBn)		506 ± 64	0.497 ± 0.059	1012	75.3 ± 0.4
46 (R ¹ = H, R ² = OH)		142 ± 16	6.06 ± 0.59	23.3	54.4 ± 6.6
47 (R ¹ = R ² = OH)		542 ± 16	35.6 ± 2.1	15.2	(*)
Tacrine		412 ± 15	44.2 ± 1.7	9.3	---
Bis(7)tacrine		0.81 ± 0.09 [31]	---	---	71.1 ± 0.7 [31]

(*) Not tested, due to significant interference (quenching of the Thioflavin T fluorescence signal)

2.2.2. Molecular modelling

Molecular modelling calculations were used to analyze the interaction between tacrine and its derivatives **43**, **45–47**, and hBuChE.

Crystallographic coordinates (PDB code: 4bds) were used as jumping-off place to study the molecular conformation of compounds **43**, **45–47** in the binding site of the enzyme. The analysis of contacts of native tacrine reveals that the main stabilization of tacrine is due to π - π stacking interactions involving the Trp82 residue (Figure 2). Two different states, protonated and non-protonated, were found for tacrine ligand. These states modify the strength of π - π interactions from -18.5 (non-protonated) to -21.9 kcal/mol (protonated). Therefore, the protonated state would be predominant at physiological pH.

The value of these interaction energies is too high for an individual π - π stacking (*ca.* 6 kcal/mol). This is because the π - π stacking interaction works together with CH- π interactions in which two protons clearly point towards the Trp aromatic ring.

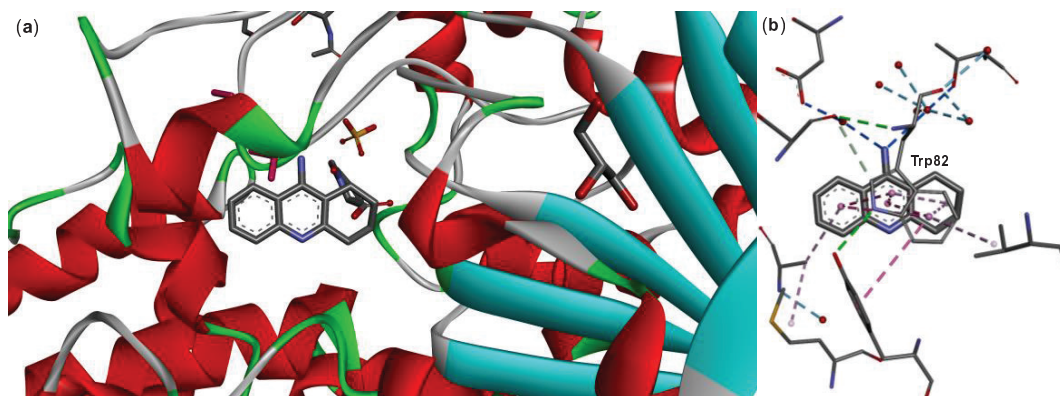


Figure 2. (a) Crystallographic coordinates of tacrine (PDB: 4bds) and (b) molecular interactions involving this compound with the binding site of BuChE

This stacking interaction of native tacrine is also found in all the derivatives subjected to modelization. However, the values of the interaction energies are slightly modified due to additional hydrophobic contacts and CH- π bonding with His438. We focused our attention on the other interactions tacrine derivatives might establish. In this context, the introduction of an alkyl chain provides enough conformational flexibility to maximize interactions.

In order to understand the role of both hydroxyl groups of hybrid **47** ($IC_{50} = 36 \pm 2$ nM), the non-covalent contacts involving this moiety were analyzed. The catechol moiety ($R_1 = R_2 = OH$) enables additional hydrogen bonding interactions (involving Gln119 and Ser287, Figure 3), and the stabilization (15.3 kcal/mol) of these combined H-bonds was estimated by means of DFT-based models.

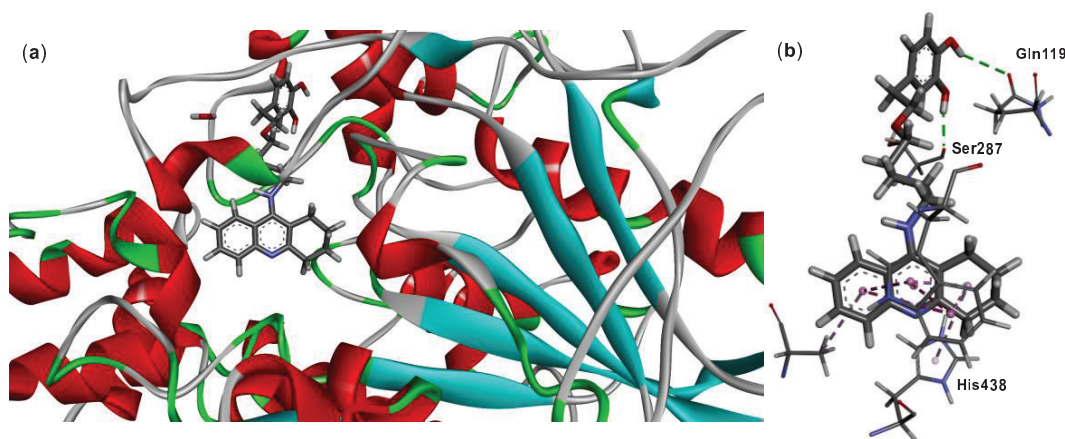


Figure 3. (a) Molecular modelling of tacrine-phenolic heterodimer **47** in the binding site of BuChE and (b) molecular interactions involving this compound. Only the main residues are shown for a better clarity.

The outcomes from molecular modelling highlighted the role of hydroxyl groups of the aromatic ring. When these hydroxyl groups are protected (OBn, compound **45**), the hydrogen bonding with Gln119 and Ser287 is broken, and an increase in the inhibition potency ($IC_{50} = 0.50 \pm 0.06$ nM) was observed. In fact, conformational flexibility allows the aromatic ring to be orientated towards the protein surface, showing intramolecular CH- π interactions and two intermolecular CH- π contacts ($\Delta E_{int} = -8.0$ kcal/mol for one of them) with Ala277 residue (Figure 4a). In addition, van der Waals interactions with residues Ile69 and Asp70 and the alkyl chain stabilize the complex.

The comparison between compound **45** and **43** ($R_1 = R_2 = OMe$, $IC_{50} = 0.515 \pm 0.050$ nM) provides information about subtle differences on active pocket. The penalty caused by hindered benzyl groups in compound **45** is balanced by aforementioned CH- π interactions, however, this kind of contacts are missing in compound **43** bearing methoxy substituents. Despite this, two new CH- π contacts are observed with Gln69-Asn68 ($\Delta E_{int} = -8.5$ kcal/mol) and Leu88-Ser89 ($\Delta E_{int} = -2.3$ kcal/mol) dipeptides moieties. Significant differences between both binding energies of CH- π contacts can be

explained from differences of computed MEP surface (-19 vs. -17 kcal/mol, respectively for each 3,4-dimethoxyphenyl face).

Remarkably, the inhibitory potency of compound **46** ($IC_{50} = 6.1 \pm 0.6$ nM) bearing a single hydroxyl group is significantly higher than that of derivative **47**. Although **46** is unable to establish the H-bond with Ser287 ($\Delta E_{\text{corr}} = -8.7$ kcal/mol), two stronger H-bond ($\Delta E_{\text{int}} = -17.5$ kcal/mol) involving the negatively charged $-\text{COO}^- \cdots \text{H}$ of Glu276, and Gln119, as well as a new NH- π contact ($\Delta E_{\text{int}} = -14.1$ kcal/mol) between the phenol ring and Asn68 (Figure 4b) are likely responsible for the stronger activity. These interactions provide a better stabilization.

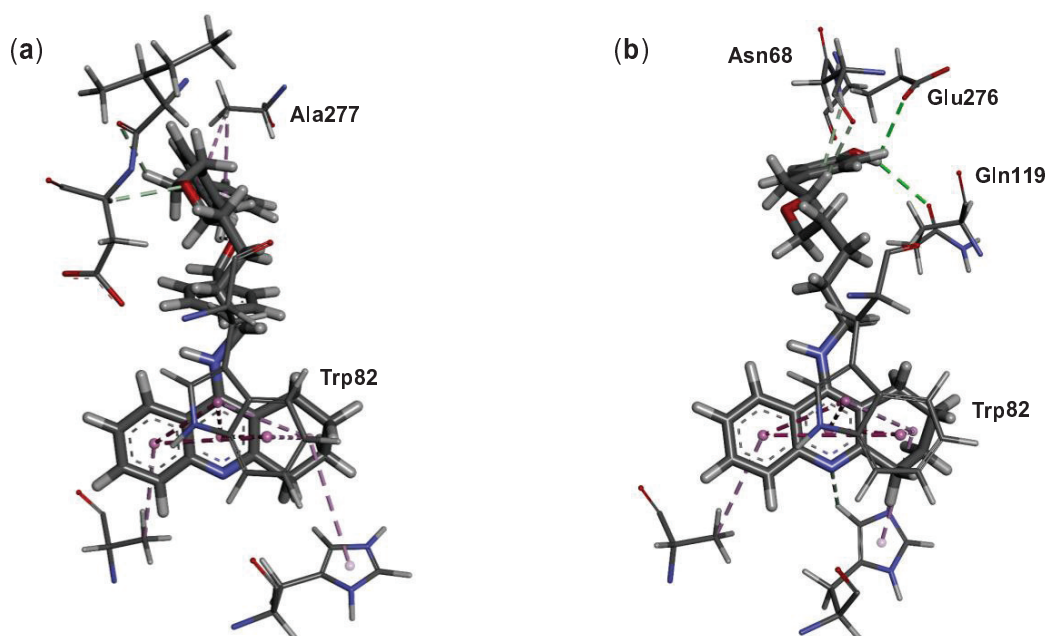


Figure 4. Protein-ligand interactions found in the interplay between BuChE and compounds **45** (a) and **46** (b). Only the main residues are shown for clarity.

In order to get further insights about the selectivity of compound **43** towards BuChE instead of AChE, we have also modeled this compound in its corresponding active site (PDB code: 4w63). Herein, compound **43** is only stabilized by non-covalent contacts involving Trp84 and His440 residues with tacrine ring. As criteria, we have considered that a better inhibition should be characterized by a more favorable binding energy value. Therefore, we have roughly estimated the overall calculated binding energy values in binding sites (Figure 5) of AChE ($\Delta E_{\text{int}} = -10.2$ kcal/mol) and BuChE

($\Delta E_{\text{int}} = -33.4$ kcal/mol). Based on these values, our results follow the similar trend of experimental selectivity index for compound **43**. The main reason seems to be the absence of interactions involving the phenolic moiety due to a short spacer regarding crystallized tacrine-based ligand of 4w63.

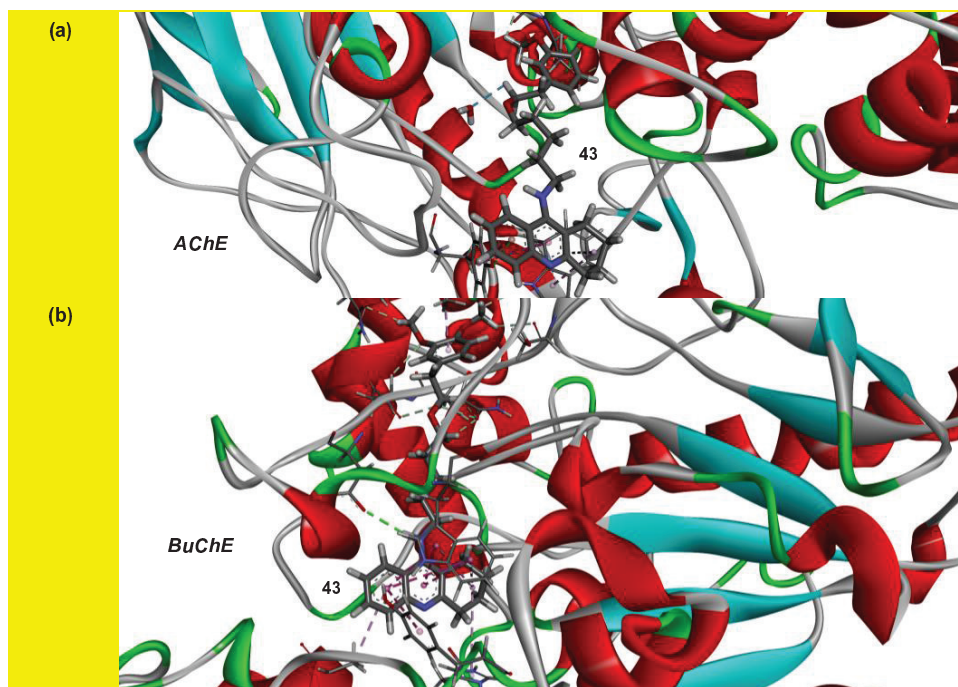


Figure 5. (a) Molecular modelling of tacrine-phenolic heterodimer **43** in the binding site of AChE and (b) modelling involving this compound and hBuChE.

2.2.4. Neuroprotection

Neurodegeneration in rat primary neurons was induced by serum and K^+ deprivation, which, upon partial ATP depletion, has been reported to cause oxidative stress and neuronal death through an apoptotic pathway [32]. This represents a good model of neuronal injury and senescence [46]; neuronal viability was determined using the MTT assay. Tacrine was used as a reference compound, and the two more potent BuChE inhibitors, **43** and **45**, were evaluated. Interestingly, only the dimethoxy derivative **43** showed relevant neuroprotective activity up to a concentration of $10 \mu\text{M}$ (Figure 6).

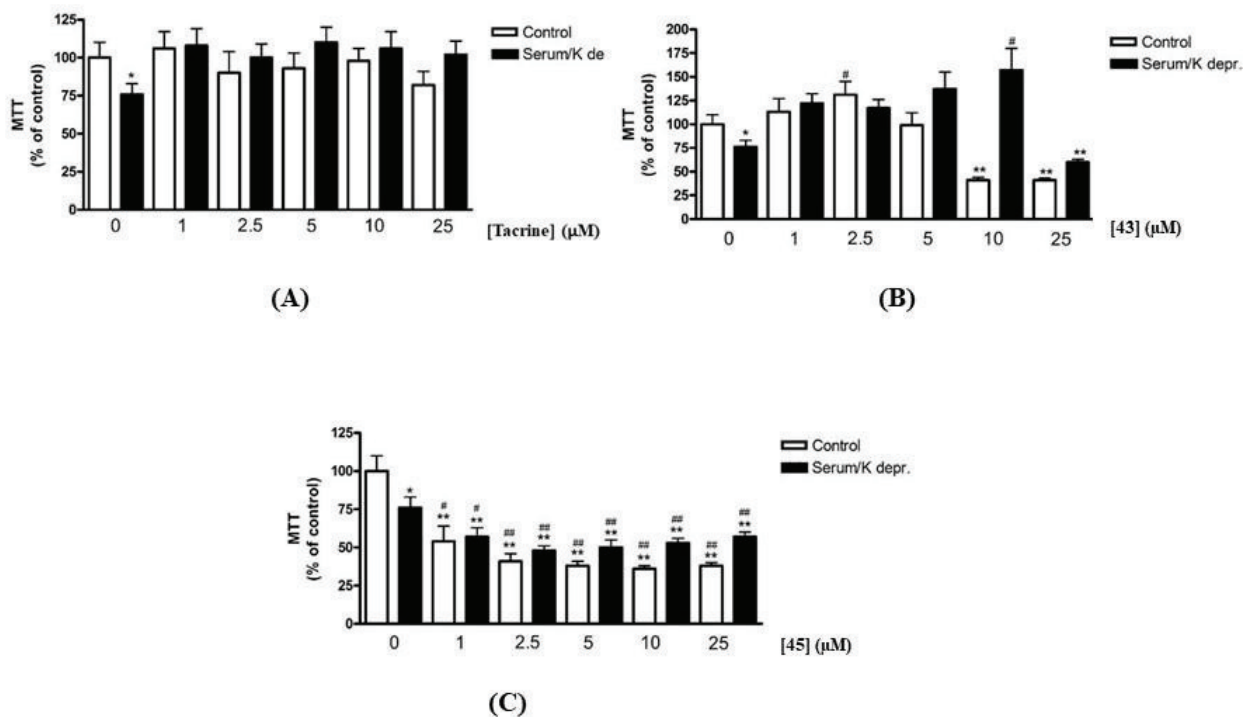


Figure 6. Neuroprotection assay (serum and K^+ deprivation) for tacrine and tacrine hybrids **43**, **45**. White bars represent control condition, whereas black bars represent serum/ K^+ deprivation in absence or presence of increasing concentrations of the tested compounds. Results are expressed as percentage of controls and are the mean \pm SE of at least 3 different experiments, each run in triplicate. * $p < 0.05$; ** $p < 0.01$ relative to control CGNs at $0\mu\text{M}$; # $p < 0.05$, ## $p < 0.01$ relative to control CGNs treated with the same concentration of the compound. Bonferroni's post-hoc test following one-way ANOVA.

2.2.3. Neurotoxicity

With these data in hand, heterodimers **43** and **45**, the most potent hBuChE inhibitors, were further tested to assess their safety profile on neurons. Thus, potential neurotoxicity against immortalized rat primary cerebellar granule neurons (CGNs; MTT viability test) was evaluated for these compounds (Figure 7). Whereas dibenzylated derivative **45** showed significant neurotoxicity even at $1\mu\text{M}$ concentration (roughly 50% of neuronal survival), dimethoxy counterpart **43** exhibited no significant neurotoxicity up to $5\mu\text{M}$.

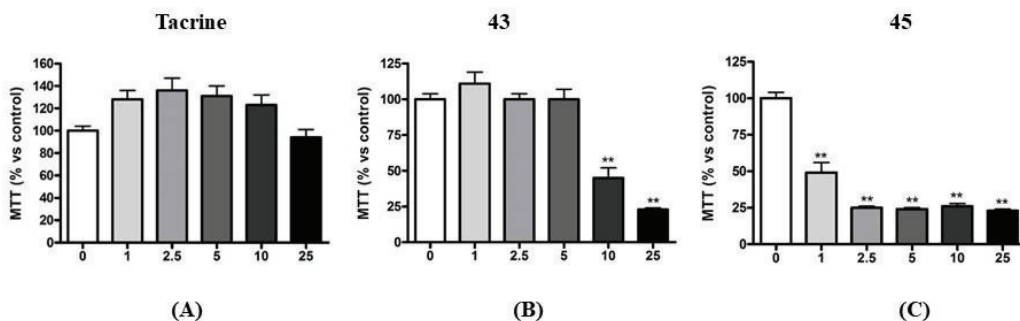


Figure 7. Neurotoxicity of tacrine (A) and tacrine-phenolic heterodimers **43** (B), **45** (C). Results are expressed as percentage of controls and are the mean \pm SE of at least 3 different experiments, each run in triplicate. **p < 0.01, ***p < 0.001 relative to control CGNs at 0 μ M. Bonferroni's post-hoc test following one-way ANOVA

We also searched for potential antiproliferative properties in a small panel of the compounds prepared herein; dual activity (inhibition of AChE-antiproliferative properties) has been reported for some marketed chemotherapeutic agents [33].

A panel of six human tumor cell lines was used, namely A549 (non-small cell lung), HBL-100 (breast), HeLa (cervix), SW1573 (non-small cell lung), as drug sensitive lines, T-47D (breast) and WiDr (colon) as drug resistant lines. Antiproliferative activities, in terms of GI₅₀ values (μ M) are depicted in Supporting Information file (Table S1). Interestingly, 9-piperidine-tetrahydroacridine **27** exhibited strong antiproliferative activity (GI₅₀ = 5.2, 4.5 μ M) against the two drug resistant lines (T-47D and WiDr); this represents an increase of activity of up to 10-fold when compared to classical chemotherapeutic agents, like 5-fluorouracil used as a reference compound. Moreover, for such lines, a selectivity index of roughly 5 was found when comparing with non-tumor cell lines (human fibroblast), in contrast with chemotherapeutic agents, which turned out to be more potent against fibroblasts than against most of the tested tumor cell lines.

2.2.4. Hepatotoxicity assessment

Hepatotoxicity of tacrine and the two tacrine-phenolic heterodimers considered as potential lead compounds in terms of anti-cholinesterases (derivatives **43** and **45**) was evaluated after 24 hours by MTT viability test (Figure 8). Whereas dibenzylated derivative **45** showed significant hepatotoxicity at all concentrations, dimethoxy

counterpart **43** exhibited a constant hepatic survival (roughly 60-70% of hepatic survival).

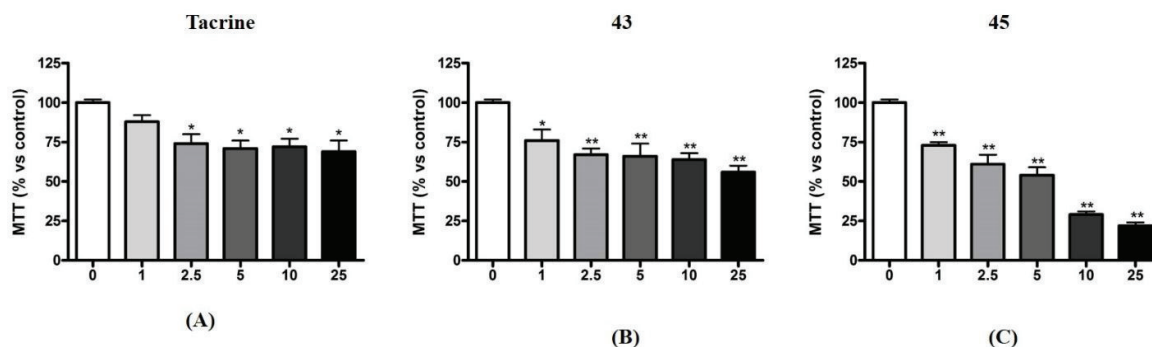


Figure 8. Hepatotoxicity of tacrine (A) and tacrine-phenolic heterodimers **43** (B), **45** (C). Results are expressed as percentage of controls and are the mean \pm SE of at least 2 different experiments, each run in duplicate. * $p < 0.05$ ** $p < 0.01$ relative to control HepG2 at 0 μ M. Bonferroni's post-hoc test following one-way ANOVA

Taken all together, data collected herein clearly indicate that compound **43** exhibits the best pharmacological profile and thus, can be considered as a valuable lead multitarget drug for the treatment of Alzheimer's disease, in contraposition of dibenzylated derivative **45**. The latter, despite the good profile concerning inhibition of BuChE and inhibition of A β deposition, exhibits significant neuro- and hepatotoxicity, as indicated by the bioassays conducted herein; as a result, compound **45** must be discarded as a potential anti-Alzheimer's agent.

2.2.5. Stability in plasma

Stability of new inhibitors in plasma is an important parameter in order to assess potential degradation which may affect *in vivo* activity. Stability of **43**, the compound with the best pharmacological profile, at 37°C in plasma was assayed using a LC-MS approach and propranolol as internal standard (IS). Three time points were considered, namely 60, 180 and 360 min. The ratio of **43** and IS peak areas at $t = 0$ and at the selected time points was compared (Figure 9). Within the selected time-frame no significant degradation was observed indicating good plasma stability for **43**, suggesting the stability of the ether-based linker under physiological conditions.

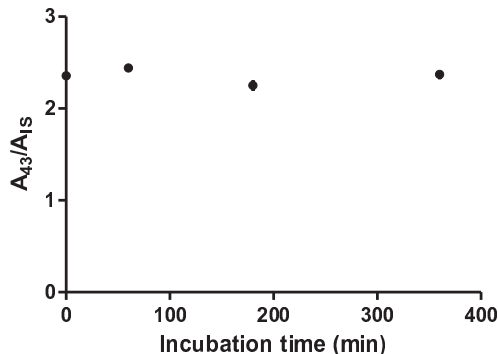


Figure 9. Plasma stability of derivative **43**. The ratio between the areas of **43** and IS is plotted as a function of the incubation time. The study was performed at 37°C using a concentration of **43** equals to 10 µM.

3. Conclusions

In conclusion, we have accomplished the preparation of a plethora of tacrine-polyphenol heterodimers, modifying the type (imino, amino, ether) and length of the tether, together with the nature and position of the substituents on the aryl core. Extensive analysis of bioactivities has revealed that the dimethoxy derivative **43** is a promising lead candidate for Alzheimer's disease treatment. This compound hits two key hallmarks of the Alzheimer's disease. Indeed, it behaves as an extremely potent and selective inhibitor of hBuChE, with activity in the subnanomolar range and inhibits to a good extent the self-aggregation of β -amyloid peptide. The inhibitory profiles against cholinesterases were explained *via* molecular modelling, by analysing the key intramolecular interactions. Compound **43** showed to be safe for neurons at concentration as high as 5 µM, and to provoke only limited hepatotoxicity at relatively high concentrations; interestingly, it exhibited neuroprotective properties in primary rat neurons, using a model in which neuronal damage was induced by serum and K⁺-deprivation, a well-validated method for reproducing neuronal injury and senescence. Moreover, its ether-type linker proved to be stable under physiological conditions.

Overall, the tacrine-dimethoxyphenyl hybrid **43** exhibits excellent properties as a novel multi-target drug for tackling Alzheimer's disease.

4. Materials and methods

4.1. Materials and methods

4.1.1. General procedures

^1H (300.1 and 500.1 MHz) and ^{13}C (75.5 and 125.7 MHz) NMR spectra were recorded at 25 °C on a Bruker Avance 300//Avance III 500 MHz spectrometers using the solvent indicated in each case. ^1H and ^{13}C assignments were confirmed by 2D COSY and HSQC experiments. Mass spectra (ESI) were recorded on a Q Exactive mass spectrometer. TLCs were performed on aluminium pre-coated sheets (E. Merck Silica gel 60 F₂₅₄); spots were visualized by UV light, and by charring with 10% vanillin in EtOH containing 1% of H₂SO₄. Column chromatography was performed using E. Merck Silica Gel 60 (40–63 μm), using the eluant indicated in each case.

4.1.2. Inhibition of cholinesterases

Ellman's assay [25] was followed with minor modifications. For non-human enzymes (AChE from *Electrophorus electricus* and BuChE from equine serum), acetyl- and butyrylthiocholines iodides were used as substrates (14.5–116 μM and 9.2–73.6 μM). Stock solutions of the inhibitor were prepared in DMSO; maximum DMSO concentration was 1.25%. Activity was monitored in 1.2-mL Polystyrene cuvettes containing 0.1 mM phosphate buffer (pH 8.0), 3 mM DTNB, different substrate concentrations (5 different concentrations), inhibitor (or solvent) plus water up to a constant volume of 1.14 mL. Reaction was started by adding 60 μL of properly diluted enzyme solution at 25 °C. The formation of the chromophore was monitored at 405 nm for 125 s. Initial rates were calculated from the slopes of the plots obtaining when representing Abs vs. t. For the calculation of the inhibition constants (K_i 's) and the mode of inhibitor, Lineweaver-Burk plot (double reciprocal plot) was used ($1/V$ vs. $1/[S]$) for 2-3 different inhibitor concentrations.

Ellman's assay was also used for estimating the activity of human enzymes [26]. Human recombinant AChE (Sigma, Italia) and BuChE from human serum (Sigma, Italia) were used for the evaluation.

4.1.3. Inhibition of $A\beta_{42}$ self-aggregation

Previously described methodology was used [26]. Inhibitors were solubilized in methanol at 2.5 mM concentration and diluted in the assay buffer. Each compound was assayed in duplicate in at least two independent experiments.

4.1.4. Molecular modelling

Human BuChE complexed with tacrine was obtained from Protein Data Bank (PDB code: 4bds) [34]. This protein was prepared with MAESTRO software suite [35]. Then, each tacrine derivative was built by modifying the tacrine moiety of 4bds structure. Analogous methodology was applied for AChE complexed with tacrine-benzofuran hybrid inhibitor (PDB code: 4w63) [36].

Molecular dynamic simulations were carried out using Chem3D program. The equilibration protocol consisted of an initial molecular mechanic minimization using MM2 force field (RMS gradient 0.01), followed by a minimization just moving the tacrine derivative (10,000 steps) whereas the system was heated at a constant volume until 300 K using a time constant for the heat bath coupling of 1 ps.

Non-covalent interactions between tacrine models and binding sites were evaluated using the crystallographic coordinates at M06-2X/def2-TZVP level of theory with Gaussian 09 package [37]. In addition, the Grimme's dispersion correction [38] was also included as implemented in Gaussian 09. The basis set superposition error for the calculation of interaction energies has been corrected using the counterpoise method [39] as followed:

$$\Delta E_{int} = E_{system} - E_1 - E_2$$

$$\Delta E_{corr} = \Delta E_{int} + E_{BSSE}$$

Models of compounds **45**, **46** and **47** were fully optimized at the same level of theory. Frequency analysis was performed to characterize these structures as minima ($N_{imag} = 0$). Solvent effects (H_2O) were evaluated during the optimization by applying the polarizable continuum model (PCM) with the integral equation formalism variant (IEFPCM).

4.1.5. Neuroprotection assays

Two different models for analyzing the potential neuroprotection exerted by tested compounds were used; in both cases, neuronal viability was quantified using the MTT (3-(4,5-dimethylthiazol-2-yl)-2,5-diphenyltetrazolium bromide) assay.

In one of such models, 6-hydroxydopamine was used as the neurotoxic agent (See Supporting Information).

In the other one, neurodegeneration was achieved by serum and K⁺-deprivation for 48 h [32,40].

4.1.6. Neurotoxicity and cytotoxicity assays

Previously described methodologies were used [26]. For the *in vitro* antiproliferative activity, the protocol of the USA National Cancer Institute (NCI), against the six human solid tumor cell lines, and the one non-tumor (BJ-hTert, human fibroblasts) with minor modifications, was followed [41].

4.17. Cell cultures for hepatotoxicity assays

Human hepatoma cell line (HepG2) was cultured in Dulbecco Modified Eagle Medium (DMEM) supplemented with 10% heat inactivated Fetal Bovine Serum (FBS), 1% Penicillin/Streptomycin and 2mM Glutamine (all cell cultures' reagents were from Aurogene Srl, Rome, Italy). At confluence, cells were trypsinized for 5 minutes at 37 °C and trypsin was inactivated with complete DMEM medium. Detached cells were then collected, centrifuged for 5 minutes at 300xg and resuspended to be counted. For the experiments, hepatocytes were plated on 96 well plates, previously coated with 10 µg/mL poly-L-lysine (Sigma-Aldrich) at the density of 2x10⁴/0.2 mL medium/well in presence or absence of increasing concentrations of the compounds (0, 1, 2.5, 5, 10 and 25 µM) in serum-free medium for 24h.

4.1.8. Determination of stability in plasma

A 5 μL aliquot of **43** stock solution (210 μM in PBS buffer) was added to 100 μL of plasma from a healthy volunteer to reach the final inhibitor concentration of 10 μM . Samples were incubated at 37°C, under gentle agitation (300 rpm, Thermomixer Comfort, Eppendorf). At selected time (0, 60, 180 and 360 min), plasma proteins were precipitated by addition of 400 μL of ice-cold acetonitrile containing propranolol as internal standard (IS, 6.25 μM). Each time point was assayed in triplicate. Samples were centrifuged at 13000 rcf for 10 min at 4°C, then, 350 μL of supernatant were collected and dried under nitrogen stream. Finally, the residue was re-suspended in 1 mL of $\text{H}_2\text{O}/\text{AcCN}$ (65/35, v/v) and analyzed by a liquid chromatography-mass spectrometry (LC-MS) approach. LC analysis was carried out by an Agilent 1200 Series (Walbronn, Germany) equipped with an autosampler. Analyses were performed on a C18 (Aeris; 150 \times 2.1 mm i.d., 3.6 μm ; Phenomenex) column thermostated at 60°C by a column oven (SICO-300 Column Oven, LabService Analytica). Mobile phase was $\text{H}_2\text{O}/\text{AcCN}/\text{FA}$, (65/35/0.1, (v/v/v)), the flow rate was set at 0.3 mL/min and the injection volume was 5 μL . Mass spectrometry analyses were performed on a Q-ToF spectrometer (Micromass, Manchester, UK) equipped with a Z-spray ion source. The ESI source temperature was set at 120 °C, the desolvation temperature at 280 °C, the capillary voltage at 3.0 kV, and the cone voltage at 35 V. Single ion monitoring (SIM) acquisitions in positive polarity were performed at 449 and 260 m/z for **43** and IS, respectively. The ratio between **43** and IS peak area was plotted against time to evaluate **43** stability in plasma.

4.2. Chemistry

4.2.1. (E)-N-(3',4'-Dimethoxybenzylidene)-1,2,3,4-tetrahydroacridin-9-amine (**6**). To a mixture of tacrine (50.0 mg, 0.25 mmol) and 3,4-dimethoxybenzaldehyde (35.9 mg, 0.21 mmol, 0.8 equiv.) in toluene (2 mL) was added diethylamine (pH 9–10). The mixture was refluxed under argon for 5 days. Afterwards it was concentrated to dryness and the residue was purified by column chromatography ($\text{CH}_2\text{Cl}_2 \rightarrow 40:1 \text{ CH}_2\text{Cl}_2\text{-MeOH}$). Yield: 35.8 mg, 49%; $R_f = 0.61$ (10:1 $\text{CH}_2\text{Cl}_2\text{-MeOH}$). $^1\text{H-NMR}$ (500 MHz, CD_3OD) δ 8.25 (s, 1H, N=CH), 7.88 (d, 1H, $J_{7,8} = 8.4$ Hz, H-8), 7.70 (brs, 1H, H-2'), 7.65 (d, 1H, $J_{5,6} = 8.4$ Hz, H-5), 7.62 (m, 1H, H-7), 7.45 (brd, 1H, $J_{5,6'} = 8.2$ Hz, H-6'), 7.38 (t, 1H, $J_{6,7} = 7.5$ Hz, H-6), 7.06 (d, 1H, H-5'), 3.91 (s, 3H, OMe), 3.90 (s, 3H, OMe), 3.07 (t,

2H, $J_{\text{H,H}} = 6.5$ Hz, H-4), 2.69 (t, 2H, $J_{\text{H,H}} = 6.5$ Hz, H-1), 1.94 (m, 2H, H-2), 1.83 (m, 2H, H-3) ppm; $^{13}\text{C-NMR}$ (125.7 MHz, CD_3OD) δ 165.6 (C-4a), 160.6 (N=CH), 157.1 (C-9), 154.6 (C-4'), 151.1 (C-3'), 147.5 (C-10a), 130.2 (C-1'), 129.8 (Ar-C), 128.0 (Ar-C), 126.5 (Ar-C), 126.0 (Ar-C), 124.1 (Ar-C), 121.9 (C-9a), 119.3 (C-8a), 112.3 (C-5), 110.8 (C-2), 56.5 (OMe), 56.5 (OMe), 34.4 (C-4), 26.2 (C-1), 23.8 (C-2, C-3) ppm; HRESI-MS calcd. for $\text{C}_{22}\text{H}_{23}\text{N}_2\text{O}_2$ ($[\text{M}+\text{H}]^+$): 347.1760, found: 347.1745.

4.2.2. (E)-N-4'-(Benzyloxybenzylidene)-1,2,3,4-tetrahydroacridin-9-amine (7). To a mixture of tacrine (39.2 mg, 0.20 mmol, 1) and 4-benzyloxybenzaldehyde (70.4 mg, 0.33 mmol, 1.7 equiv.) in toluene (2 mL) was added diethylamine (pH 9-10). The mixture was refluxed under argon for 48 h. Afterwards, it was concentrated to dryness and the residue was purified by column chromatography (cyclohexane \rightarrow 1:2 EtOAc–cyclohexane). Yield: 50.2 mg, 65%; $R_f = 0.41$ (1:1 EtOAc–cyclohexane). $^1\text{H-NMR}$ (300 MHz, CDCl_3) δ 8.22 (s, 1H, N=CH), 7.97 (d, 1H, $J_{7,8} = 8.6$ Hz, H-8), 7.92 (m, 2H, H-2', H-6'), 7.67 (td, 1H, $J_{5,6} = J_{6,7} = 8.5$ Hz, $J_{6,8} = 0.8$ Hz, H-6), 7.60 (ddd, 1H, $J_{5,7} = 1.5$ Hz, H-7), 7.49–7.32 (m, 6H, Ar-H), 7.12 (m, 2H, H-3', H-5'), 5.18 (s, 2H, OCH_2), 3.14 (t, 2H, $J_{\text{H,H}} = 6.4$ Hz, H-4), 2.72 (t, 2H, $J_{\text{H,H}} = 6.4$ Hz, H-1), 1.96 (m, 2H, H-2), 1.86 (m, 2H, H-3) ppm; $^{13}\text{C-NMR}$ (75.5 MHz, CDCl_3) δ 162.7, 162.2 (C-4a, C-4'), 159.5 (N=CH), 155.0 (C-9), 147.0 (C-10a), 136.5 (C-1''), 130.9, 128.9, 128.8, 128.7, 128.5, 128.4, 127.6, 125.1, 123.1, 120.6, 118.0 (Ar-C), 115.4 (C-3', C-5'), 70.3 (OCH_2), 34.3 (C-4), 25.4 (C-1), 23.2, 23.0 (C-2, C-3) ppm; HRESI-MS calcd. for $\text{C}_{27}\text{H}_{25}\text{N}_2\text{O}_2$ ($[\text{M}+\text{H}]^+$): 393.1967, found: 393.1953.

4.2.3. (E)-N-[3',4'-Bis(benzyloxy)benzylidene]-1,2,3,4-tetrahydroacridin-9-amine (8). To a mixture of tacrine (40.0 mg, 0.20 mmol) and 3,4-dibenzyloxybenzaldehyde (108.4 mg, 0.34 mmol, 1.7 equiv.) in toluene (2 mL) was added diethylamine (pH 9-10). The mixture was refluxed under argon for 44 hours. After that, it was concentrated to dryness and the residue was purified by column chromatography (cyclohexane \rightarrow 1:1 EtOAc–cyclohexane). Yield: 56.6 mg, 56%; $R_f = 0.36$ (1:1 EtOAc–cyclohexane). $^1\text{H-NMR}$ (300 MHz, CDCl_3) δ 8.16 (s, 1H, N=CH), 7.98 (d, 1H, $J_{7,8} = 8.2$ Hz, H-8), 7.80 (brs, 1H, H-2'), 7.65 (dd, 1H, $J_{5,6} = 8.4$ Hz, $J_{5,7} = 0.9$ Hz, H-5), 7.60 (ddd, 1H, $J_{6,7} = 8.4$ Hz, $J_{6,8} = 1.5$ Hz, H-6), 7.50 (m, 4H, Ar-H), 7.37 (m, 8H, Ar-H), 7.02 (d, 1H, $J_{5',6'} = 8.2$ Hz, H-5'), 5.27 (s, 4H, 2OCH_2), 3.15 (t, 2H, $J_{\text{H,H}} = 6.7$ Hz, H-4), 2.71 (t, 2H, $J_{\text{H,H}} = 6.5$ Hz, H-1), 1.96 (m, 2H, H-2), 1.86 (m, 2H, H-3) ppm; $^{13}\text{C-NMR}$ (75.5 MHz, CDCl_3) δ

162.8 (C-4a), 159.5 ppm (N=CH), 154.8, 152.6 (C-9, C-4'), 149.5 (C-3'), 147.0 (C-10a), 136.9, 136.7, 129.1, 128.7, 128.7, 128.5, 128.1, 128.1, 127.6, 127.2, 125.1, 124.9, 123.0, 120.5, 118.0 (Ar-C), 113.8, 112.5 (C-2, C-5), 71.2 (OCH₂), 71.1 (OCH₂), 34.3 (C-4), 25.4 (C-1), 23.2 (C-2), 23.0 (C-3) ppm; HRESI-MS calcd. for C₃₄H₃₁N₂O₂ ([M+H]⁺): 499.2386, found: 499.2372.

4.2.4. (E)-N-[3',4',5'-Tris(benzyloxy)benzylidene]-1,2,3,4-tetrahydroacridin-9-amine (**9**). To a mixture of tacrine (30.9 mg, 0.16 mmol) and 3,4,5-tribenzyloxybenzaldehyde (112.7 mg, 0.26 mmol, 1.7 equiv.) in toluene (2 mL) was added diethylamine (pH = 9–10). Then, it was refluxed under argon for 45 h. After that, the crude reaction mixture was concentrated to dryness and the residue was purified by column chromatography (cyclohexane → 1:1 EtOAc–cyclohexane). Yield: 54.4 mg, 58%; R_f = 0.37 (1:1 EtOAc–cyclohexane). ¹H-NMR (300 MHz, CDCl₃) δ 8.16 (s, 1H, N=CH), 8.00 (d, 1H, J_{7,8} = 8.2 Hz, H-8), 7.63 (m, 2H, H-5, H-6), 7.48–7.30 (m, 18H, Ar-H), 5.21 (s, 4H, 2OCH₂), 5.19 (s, 2H, OCH₂), 3.16 (t, 1H, J_{3,4} = 6.4 Hz, H-4), 2.72 (t, 2H, J_{1,2} = 6.4 Hz, H-1), 1.98 (m, 2H, H-2), 1.88 (m, 2H, H-3) ppm; ¹³C-NMR (75.5 MHz, CDCl₃) δ 163.0 (Ar-C), 159.5 (N=CH), 154.5, 153.4, 147.0, 142.1, 137.6, 136.8, 130.9, 128.8, 128.7, 128.5, 128.4, 128.2, 128.1, 127.6, 125.2, 123.0, 120.4, 117.9 (Ar-C), 108.3 (C-2', C-6'), 75.4 (OCH₂), 71.4 (OCH₂), 34.2 (H-4), 25.5 (H-1), 23.1, 23.0 (H-2, H-3) ppm; HRESI-MS calcd. for C₄₁H₃₇N₂O₃ ([M+H]⁺): 605.2804, found: 605.2776.

4.2.5. (E)-N-(4'-Hydroxybenzylidene)-1,2,3,4-tetrahydroacridin-9-amine (**11**). A mixture of **7** (39.1 mg, 0.10 mmol) and Pd(OH)₂ (19.2 mg) in 1:1 CH₂Cl₂–MeOH (2 mL) was hydrogenated at rt and 1 atm for 30 min. Afterwards, it was filtrated through a Celite® pad and concentrated to dryness. The residue was purified by column chromatography (60:1 CH₂Cl₂–MeOH → 20:1 CH₂Cl₂–MeOH). Yield: 14.3 mg, 48%; R_f = 0.46 (10:1 CH₂Cl₂–MeOH). ¹H-NMR (300 MHz, CD₃OD–CDCl₃) δ 8.20 (s, 1H, N=CH), 7.88 (d, 1H, J_{7,8} = 8.3 Hz, H-8), 7.82 (m, 2H, H-2', H-6'), 7.67 (dd, 1H, J_{5,6} = 8.4 Hz, J_{5,7} = 1.0 Hz, H-5), 7.61 (ddd, 1H, J_{6,8} = 1.4 Hz, H-6), 7.38 (ddd, 1H, H-7), 6.94 (m, 2H, H-3', H-5'), 3.09 (t, 2H, J_{H,H} = 6.8 Hz, H-4), 2.72 (t, 2H, J_{H,H} = 6.8 Hz, H-1), 1.96 (m, 2H, H-2), 1.86 (m, 2H, H-3) ppm.; ¹³C-NMR (125.7 MHz, CD₃OD–CDCl₃) δ 164.8, 162.5, 160.0 (C-4a, C-4', N=CH), 156.7 (C-9), 146.8 (C-10a), 131.9 (Ar-C),

129.9, 127.7, 127.5, 126.1, 123.8, 121.5, 119.1 (Ar-C), 116.6 (C-3', C-5'), 33.9 (C-4), 25.8 (C-1), 23.4 (C-2), 23.4 (C-3) ppm; HRESI-MS calcd. for C₂₀H₁₉N₂O ([M+H]⁺): 303.1497, found: 303.1492.

4.2.6. N-[4'-(Hydroxyphenyl)methyl]-1,2,3,4-tetrahydroacridin-9-amine (**12**). A mixture of **7** (53.0 mg, 0.14 mmol) and Pd/C (29.1 mg) in 1:1 CH₂Cl₂-MeOH (2 mL) was hydrogenated at rt and 1 atm for 3 h. Afterwards, it was filtrated through a Celite® pad and concentrated to dryness. The residue was purified by column chromatography (10:1 CH₂Cl₂-MeOH → 5:1 CH₂Cl₂-MeOH). Yield: 11.7 mg, 29%; R_f = 0.27 (5:1 CH₂Cl₂-MeOH). ¹H-NMR (300 MHz, CD₃OD) δ 8.26 (d, 1H, J_{7,8} = 8.4 Hz, H-8), 7.74 (m, 2H, H-4, H-5), 7.42 (m, 1H, H-6), 7.18 (m, 2H, H-2', H,6'), 6.78 (m, 2H, H-3', H-5'), 4.94 (s, 2H, N-CH₂), 3.01 (m, 2H, H-4), 2.72 (m, 2H, H-1), 1.94 (m, 4H, H-2, H-3) ppm; ¹³C-NMR (75.5 MHz, CD₃OD) δ 158.2, 156.0 (C-4a, C-4', C-9), 153.8 (C-10a), 133.0, 130.4 (Ar-C), 129.2 (C-2', C-6') 126.3, 125.9, 122.1 (Ar-C), 116.7 (C-3', C-5'), 114.4 (Ar-C), 52.0 (N-CH₂), 30.6 (C-4), 25.1 (C-1), 23.2 (C-2), 22.3 (C-3) ppm; HRESI-MS calcd. for C₂₀H₂₁N₂O ([M+H]⁺): 305.1654, found: 305.1648.

4.2.7. (E)-N-[3',4'-(Dihydroxy)benzylidene]-1,2,3,4-tetrahydroacridin-9-amine (**13**) and N-[3',4'-(Dihydroxy)phenyl)methyl]-1,2,3,4-tetrahydroacridin-9-amine (**14**). A mixture of **8** (53.1 mg, 0.11 mmol) and Pd(OH)₂ (24.5 mg) in 1:1 CH₂Cl₂-MeOH (3 mL) was hydrogenated at rt and 1 atm for 1.5. After that, it was filtrated through a Celite® pad and concentrated to dryness. The residue was purified by column chromatography (40:1 CH₂Cl₂-MeOH → 5:1 CH₂Cl₂-MeOH) to give **13** and **14**.

Eluted first was **13**. Yield: 6.8 mg, 20%; R_f = 0.35 (10:1 CH₂Cl₂-MeOH). ¹H-NMR (500 MHz, CD₃OD-CDCl₃) δ 8.10 (s, 1H, N=CH), 7.87 (d, 1H, J_{7,8} = 8.4 Hz, H-8), 7.66 (dd, 1H J_{5,6} = 8.4 Hz, J_{5,7} = 1.0 Hz, H-5), 7.59 (t 1H, J_{6,7} = 8.4 Hz, H-6), 7.50 (brd, 1H, J_{2',6'} = 1.5 Hz, H-2'), 7.36 (t, 1H, H-7), 7.23 (dd, 1H, J_{5,6} = 8.2 Hz, H-6'), 6.91 (d, 1H, H-5'), 3.07 (brt, 2H, J_{H,H} = 6.4 Hz, H-4), 2.70 (brt, 2H, J_{H,H} = 6.5 Hz, H-1), 1.94 (m, 2H, H-2), 1.83 (m, 2H, H-3) ppm; ¹³C-NMR (125.7 MHz, CD₃OD-CDCl₃) δ 164.7 (N=CH), 159.8 (C-4a), 156.2 (C-9), 150.6 (C-4'), 146.7, 146.2 (C-10a, C-3'), 129.6 (C-8), 127.9 (C-1'), 127.4, 125.8 (C-5, C-6), 124.1 (C-5), 123.5 (C-6'), 121.3, 118.9 (C-8a,

C-9a), 115.8 (C-5'), 114.7 (C-2'), 33.7 (C-4), 25.6 (C-1), 23.2 (C-2, C-3) ppm; HRESI-MS calcd. for C₂₀H₁₉N₂O₂ ([M+H]⁺): 319.1447, found: 319.1435.

Eluted second was **14**. Yield: 18.7 mg, 55%; R_f = 0.19 (5:1 CH₂Cl₂-MeOH). ¹H-NMR (300 MHz, CD₃OD) δ 8.25 (d, 1H, J_{7,8} = 8.5 Hz, H-8), 7.73 (m, 2H, H-5, H-6), 7.41 (td, 1H, J_{6,7} = J_{7,8} = 8.2 Hz, J_{5,7} = 2.0 Hz, H-7), 6.77 (d, 1H, J_{2',6'} = 2.1 Hz, H-2'), 6.75 (d, 1H, J_{5',6'} = 8.1 Hz, H-5'), 6.68 (dd, 1H, H-6'), 4.88 (s, 2H, N-CH₂), 3.00 (m, 2H, H-4), 2.72 (m, 2H, H-1), 1.93 (m, 4H, H-2, H-3) ppm; ¹³C-NMR (75.5 MHz, CD₃OD) δ 157.3, 153.0, 146.9, 146.1, 133.3, 130.8, 126.5, 125.9, 121.3, 119.1, 117.6, 116.7, 114.8, 113.8 (Ar-C), 51.8 (N-CH₂), 30.1 (C-4), 25.0 (C-1), 23.1 (C-2), 22.1 (C-3) ppm; HRESI-MS calcd. for C₂₀H₂₁N₂O₂ ([M+H]⁺): 321.1603, found: 321.1589.

4.2.8. (E)-N-(3',4',5'-Trihydroxybenzylidene)-1,2,3,4-tetrahydroacridin-9-amine (**15**).

A mixture of **9** (45.9 mg, 0.076 mmol) and Pd/C (24.5 mg) in 1:1 CH₂Cl₂-MeOH (2 mL) was hydrogenated at rt and 1 atm for 2 h. After that, it was filtrated through a Celite® pad and concentrated to dryness. The residue was purified by column chromatography (CH₂Cl₂ → 5:1 CH₂Cl₂-MeOH). Yield: 12.7 mg, 50%; R_f = 0.58 (5:1 CH₂Cl₂-MeOH). ¹H-NMR (300 MHz, CD₃OD) δ 8.07 (s, 1H, N=CH), 7.88 (d, 1H, J_{7,8} = 8.4 Hz, H-8), 7.65 (m, 2H, H-5, H-6), 7.41 (td, 1H, J_{6,7} = 8.3 Hz, J_{5,7} = 1.1 Hz, H-7), 7.03 (s, 2H, H-2', H-6'), 3.09 (t, 2H, J_{H,H} = 6.5 Hz, H-4), 2.70 (t, 2H, J_{H,H} = 6.5 Hz, H-1), 1.96 (m, 2H, H-2), 1.86 (m, 2H, H-3) ppm; ¹³C-NMR (125.7 MHz, CD₃OD) δ 165.9, 160.5 (Ar-C, N=CH), 157.5, 147.3, 147.2, 134.2, 130.3, 127.8, 127.6, 126.5, 124.2, 122.0, 119.4 (Ar-C), 109.5 (C-2', C-6'), 34.3 (C-4), 26.1 (C-1), 23.8 (C-2, C-3) ppm; HRESI-MS calcd. for C₂₀H₁₉N₂O₃ ([M+H]⁺): 335.1396, found: 335.1390.

4.2.9. 2-(4'-Benzyloxy)phenethyl-p-methylbenzenesulfonate (**17a**). To a solution of 2-(4'-benzyloxyphenyl)ethanol (790 mg, 3.46 mmol) in CH₂Cl₂ (10 mL) were added TsCl (815 mg, 4.27 mmol, 1.2 equiv.) and Et₃N (0.6 mL, 4.30 mmol, 1.2 equiv.), and the corresponding mixture was refluxed for 18 hours. After that, it was concentrated to dryness under reduced pressure, and the residue was purified by flash column chromatography (CH₂Cl₂ → toluene → Et₂O) to afford **17a**. Yield: 590 mg, 44%. ¹H-NMR (300 MHz, CDCl₃) δ 7.61 (m, 2H, Ar-H_o, Ts), 7.37-7.18 (m, 7H, Ar-H), 6.94 (m, 2H, H-2', H-6'), 6.78 (m, 2H, H-3', H-5'), 4.96 (s, 2H, CH₂-Ar), 4.09 (t, 2H, J_{H,H} = 7.1

Hz, CH₂O), 2.81 (t, 2H, CH₂-Ar), 2.35 (s, 3H, CH₃-Ar) ppm; ¹³C-NMR (125.7 MHz, CDCl₃) δ 157.9 (C-4'), 144.8 (C-1, Ts), 137.1 (C-4, Ts), 133.2 (C-1'', Bn), 130.1, 129.9 (Ar-C), 128.7 (C-1'), 128.6 (Ar-C), 128.1 (C-4'', Bn), 127.9, 127.6 (Ar-C), 115.1 (C-3', C-5'), 71.0, 70.2 (CH₂O^{Ph}, CH₂O^{Ts}), 34.6 (CH₂Ar), 21.8 (CH₃Ar) ppm; HRESI-MS calcd for C₂₂H₂₂NaO₄S ([M+Na]⁺): 405.1131, found: 405.1131.

4.2.10. *1-(2'-Azidoethyl)-4-(benzyloxy)benzene (17b)*. To a solution of **17a** (631 mg, 1.65 mmol) DMSO (4 mL) was added NaN₃ (129 mg, 1.98 mmol, 1.2 equiv). After 2 hours stirring at 45°C, water (15 mL) was added, and the mixture was extracted with toluene (3x20 mL). The combined organic layers were dried over Na₂SO₄ and the solvent was eliminated under reduced pressure to give pure **17b** as a yellow solid. Yield: 401 mg, 96%. ¹H-NMR (300 MHz, CDCl₃) δ 7.46-7.33 (m, 5H, Ar-H), 7.14 (m, 2H, H-2, H-6), 6.94 (m, 2H, H-3, H-5), 5.06 (s, 2H, CH₂-OAr), 3.47 (t, 2H, J_{H,H} = 7.2 Hz, CH₂-Ar), 2.85 (t, 2H, CH₂-N₃) ppm; ¹³C-NMR (125.7 MHz, CDCl₃) δ 157.8 (C-4), 137.2 (C-1''), 130.5 (C-1), 129.9, 128.7, 128.1, 127.6 (Ar-C), 115.2 (C-3, C-5), 70.2 (CH₂O), 52.8 (CH₂N₃), 34.6 (CH₂Ar) ppm. HRESI-MS calcd for C₁₅H₁₅N₃NaO ([M+Na]⁺): 276.1107, found: 277.1110.

4.2.11. *2-(4'-Benzyloxyphenyl)ethylamine (18a)*. To a solution of **17b** (381 mg, 1.50 mmol) in anhydrous THF (7.5 mL) under Ar was added PPh₃ (521 mg, 1.99 mmol, 1.3 equiv.), and the mixture was stirred at rt for 7 h. After that, water (0.5 mL) was added and it was kept at rt for further 12 h, and then it was concentrated to dryness. The residue was purified by flash column chromatography (5:1 CH₂Cl₂-MeOH → 5:1:0.1 CH₂Cl₂-MeOH-aq. NH₃) to afford **18a** as a white solid. Yield: 293 mg, 86%.

4.2.12. *N-(4'-(benzyloxy)phenethyl)-1,2,3,4-tetrahydroacridin-9-amine (19a)*. A mixture of 9-chloro-1,2,3,4-tetrahydroacridine **16** (340 mg, 1.56 mmol, 1.3 equiv.), **18a** (273 mg, 1.20 mmol), and NaI (55 mg, 0.37 mmol, 0.31 equiv.) in phenol (2.0 g) was refluxed for 4 h. After that, it was partitioned between CH₂Cl₂ (50 mL) and 1M NaOH (3x50 mL). The organic layer was separated, dried over Na₂SO₄ and concentrated to dryness. The residue was purified by flash column chromatography (CH₂Cl₂ → 10:1 CH₂Cl₂-MeOH 10:1) to give **19a** as a green oil. Yield: 134 mg, 27%. ¹H-NMR (300

MHz, CDCl₃) δ 7.96 (d, 1H, $J_{7,8}$ = 8.4 Hz, H-8), 7.86 (d, 1H, $J_{5,6}$ = 8.5 Hz, H-5), 7.56 (m, 1H, Ar-H), 7.46-7.28 (m, 6H, Ar-H), 7.13 (m, 2H, H-2', H-6'), 6.94 (m, 2H, H-3', H-5'), 5.06 (s, 1H, CH₂O), 4.11 (m, 1H, NH), 3.76 (t, 2H, $J_{H,H}$ = 6.7 Hz, CH₂), 3.07 (t, 2H, $J_{H,H}$ = 6.1 Hz, CH₂), 2.90 (t, 2H, $J_{H,H}$ = 6.8 Hz, CH₂), 2.48 (t, 2H, $J_{H,H}$ = 6.1 Hz, CH₂), 1.86 (m, 4H, 2CH₂) ppm; ¹³C-NMR (125.7 MHz, CDCl₃) δ 158.1, 157.8 (C-4a, C-4'), 150.9, 146.9 (C-1, C-10a), 137.1, 130.6, 129.9, 128.7, 128.3, 128.1, 127.5, 123.9, 122.9 (Ar-C), 120.1 (C-8a), 116.1 (C-9a), 115.3 (C-2', C-5'), 70.2 (CH₂O), 50.3 (CH₂-NH), 36.5, 33.7, 24.6, 23.0, 22.7 (CH₂) ppm; HRESI-MS calcd for C₂₈H₂₈N₂O ([M+H]⁺): 409.2274, found: 409.2272.

4.2.13. N-[3',4'-Bis(benzyloxy)phenethyl]-1,2,3,4-tetrahydroacridin-9-amine (**19b**). To a solution of 9-chloro-1,2,3,4-tetrahydroacridine **17** (192.9 mg, 0.89 mmol, 4.7 equiv) in phenol (1.0 g) as added per-*O*-benzyldopamine **18** (64.7 mg, 0.19 mmol, 1.0 equiv.) and NaI (21.2 mg, 0.14 mmol, 0.47 equiv). The resulting mixture was refluxed for 3.5 hours; after that, it was partitioned between 1M NaOH and CH₂Cl₂. The organic layer was separated and concentrated to dryness, and the residue was purified by column chromatography (CH₂Cl₂ → 10:1 CH₂Cl₂-MeOH). Yield: 102.6 mg, quant.; R_f = 0.30 (10:1 CH₂Cl₂-MeOH). ¹H-NMR (500 MHz, (CD₃)₂CO) δ 8.11 (d, 1H, $J_{7,8}$ = 8.5 Hz, H-8), 7.96 (d, 1H, $J_{5,6}$ = 8.5 Hz, H-5), 7.59 (m, 1H, Ar-H), 7.49 (m, 1H, Ar-H), 7.48 (m, 1H, Ar-H) 7.45 (m, 1H, Ar-H) 7.44 (m, 1H, Ar-H) 7.32 (m, 7H, Ar-H), 6.96 (d, 1H, $J_{5',6'}$ = 8.0 Hz, H-5'), 6.94 (d, 1H, $J_{2',6'}$ = 2.0 Hz, H-2'), 6.77 (dd, 1H, H-6'), 5.35 (s, 1H, NH), 5.12 (s, 2H, s, CH₂-Ph), 5.03 (s, 2H, CH₂-Ph), 3.89 (m, 2H, CH₂), 2.99 (t, 2H, $J_{H,H}$ = 6.3 Hz, CH₂) 2.94 (t, 2H, $J_{H,H}$ = 7.0 Hz, CH₂), 2.59 (t, 2H, $J_{H,H}$ = 6.3 Hz, CH₂), 1.82 (m, 4H, 2CH₂) ppm; ¹³C-NMR (125.7 MHz, (CD₃)₂CO) δ 157.1, 152.9, 150.1, 148.7, 146.0, 138.8, 138.6, 133.1, 129.8, 129.2, 128.5, 128.5, 128.4, 128.3, 127.3, 124.6, 124.4, 122.6, 120.3 (Ar-C), 116.6, 116.2, 116.0 (C-2'', C-5'', C-9a), 77.8 (Ph-CH₂), 77.6 (Ph-CH₂), 50.7 (CH₂-NH), 37.2, 33.2, 25.3, 23.5, 23.0 (CH₂) ppm; HRESI-MS calcd. for C₃₅H₃₅N₂O₂ ([M+H]⁺): 515.2687, found: 515.2693.

4.2.1.4. N-(4'-Hydroxyphenethyl)-1,2,3,4-tetrahydroacridine-9-amine (**20a**). A mixture of **19a** (37 mg, 0.09 mmol), AcOH (a few drops) and Pd(OH)₂ (20 mg) in MeOH (5 mL) was hydrogenated at rt and 1 atm for 2 h. After that, it was filtrated through a Celite® pad and concentrated to dryness to give pure **20a** as a green oil. Yield: 24 mg,

84%. ¹H-NMR (300 MHz, CD₃OD) δ 8.28 (d, 1H, *J*_{7,8} = 8.6 Hz, H-8), 7.81–7.72 (m, 2H, H-5, H-6), 7.53 (m, 1H, H-7), 6.95 (m, 2H, H-2', H-6'), 6.62 (m, 2H, H-3', H-5'), 4.10 (t, 2H, *J*_{H,H} = 6.8 Hz, N-CH₂), 2.94 (m, 4H, 2CH₂), 2.51 (m, 2H, CH₂), 1.90 (m, 4H, 2CH₂) ppm; ¹³C-NMR (125.7 MHz, CD₃OD) δ 157.7, 157.4 (C-4a, C-4'), 152.8, 140.8 (C-9, C-10a), 133.4 (Ar-C), 131.0 (C-2', C-6'), 129.7, 126.1, 121.2, 117.9 (Ar-C), 116.3 (C-3', C-5'), 113.8 (C-9a), 54.8, 50.7, 36.8, 29.9, 24.9, 23.0, 22.0 ppm. HRESI-MS calcd for C₂₁H₂₃N₂O ([M+H]⁺): 319.1805, found: 319.1805.

4.2.15. **N-(3',4'-Dihydroxyphenethyl)-1,2,3,4-tetrahydroacridine-9-amine (20b).** A mixture of **19** (16.0 mg, 0.031 mmol) and Pd/C (9.8 mg) in 1:1 CH₂Cl₂–MeOH (2 mL) was hydrogenated at rt and **1** atm for 4.5 h. After that, it was filtrated through a Celite® pad and concentrated to dryness. The residue was purified by column chromatography (CH₂Cl₂ → 5:1 CH₂Cl₂–MeOH). Yield: 2.1 mg, 20%; *R*_f = 0.30 (10:1 CH₂Cl₂–MeOH). ¹H-NMR (300 MHz, CD₃OD) δ 8.31 (d, 1H, *J*_{7,8} = 8.5 Hz, H-8), 7.78 (m, 2H, H-5, H-6), 7.55 (m, 1H, H-7), 6.57 (d, 1H, *J*_{5',6'} = 7.3 Hz, H-5'), 6.53 (d, 1H, *J*_{2',6'} = 1.9 Hz, H-2'), 6.43 (dd, 1H, H-6'), 4.13 (t, 2H, *J*_{H,H} = 6.8 Hz, N-CH₂), 2.96 (m, 2H, CH₂), 2.89 (t, 2H, *J*_{H,H} = 6.8 Hz, CH₂), 2.52 (m, 2H, CH₂), 1.90 (m, 2H, CH₂) ppm; ¹³C-NMR (125.7 MHz, CD₃OD) δ 166.9, 133.2, 129.0, 127.6, 124.7, 125.7, 121.0, 120.1, 117.5, 116.6, 115.9 (Ar-C), 50.4, 36.6, 30.4, 29.1, 24.6, 22.6, 21.0 ppm; HRESI-MS calcd. for C₂₁H₂₃N₂O₂ ([M+H]⁺): 335.1754, found: 335.1754.

4.2.16. **9-(Pyrrolidin-1'-yl)-1,2,3,4-tetrahydroacridine (25).** A mixture of tacrine (200.1 mg, 1.0 mmol), 1,4-dibrombutane (0.41 mL, 3.41 mmol, 3.4 equiv.) and KOH (225.8 mg, 3.42 mmol, 3.4 equiv.) in acetonitrile (10 mL) was stirred under argon at rt for 25 h. After that, the crude reaction mixture was concentrated to dryness and the residue was partitioned between H₂O (30 mL) and EtOAc (3x30 mL). The organic layer was concentrated to dryness and then, partitioned between Et₂O (30 mL) and 6M HCl (30 mL). The aqueous layer was then neutralized with 3M NaOH (150 mL) and extracted with EtOAc (2x100 mL); the organic layer was dried with Na₂SO₄, filtered, and concentrated to dryness. The residue was purified by column chromatography (cyclohexane → 3:2 EtOAc–cyclohexane). Yield: 106.1 mg, 42%; *R*_f = 0.78 (6:4:1 EtOAc–cyclohexane–Et₃N). ¹H-NMR (300 MHz, CD₃OD) δ 7.93 (d, 1H, *J*_{7,8} = 8.4 Hz,

H-8), 7.85 (d, 1H, $J_{5,6} = 8.2$ Hz, H-5), 7.56 (t, 1H, $J_{6,7} = 8.2$ Hz, H-6), 7.40 (t, 1H, H-7), 3.39 (m, 4H, 2CH₂-N), 3.03 (t, 2H, $J_{H,H} = 6.5$ Hz, H-4), 2.81 (t, 2H, $J_{H,H} = 6.5$ Hz, H-1), 2.10 (m, 4H, H-2, H-3), 1.91 (m, 2H, CH₂), 1.82 (m, 2H, CH₂) ppm; ¹³C-NMR (75.5 MHz, CD₃OD) δ 161.2 (C-4a), 153.3 (C-9), 148.4 (C-10a), 130.0, 129.7, 128.5, 127.4, 126.0, 125.2 (Ar-C), 52.3 (CH₂-N), 34.3 (H-4), 27.4 (H-1), 23.9, 23.8 (CH₂) ppm; HRESI-MS calcd. for C₁₇H₂₁N₂ ([M+H]⁺): 253.1699, found: 253.1695

4.2.17. *9-(Piperidin-1'-yl)-1,2,3,4-tetrahydroacridine (27)*. A mixture of tacrine (400.3 mg, 2.02 mmol), 1,5-dibromopentane (0.96 mL, 6.83 mmol, 3.4 equiv.) and KOH (452.2 mg, 6.85 mmol, 3.4 equiv.) in acetonitrile (20 mL) was stirred under argon at rt for 23 h. After that, the mixture was concentrated to dryness, and the residue was partitioned between H₂O (30 mL) and EtOAc (3x30 mL). The organic layer was concentrated to dryness and then, partitioned between Et₂O (30 mL) and 6M HCl (30 mL). The aqueous layer was then neutralized with 3M NaOH (150 mL) and extracted with EtOAc (2x100 mL); the organic layer was dried over Na₂SO₄, filtered, and concentrated to dryness. The residue was purified by column chromatography (Cyclohexane → 3:2 EtOAc-cyclohexane) to give **26** (312.8 mg, 45%) and **27** (161.0 mg, 30%)

Data for **27**: $R_f = 0.76$ (6:4:1 EtOAc-cyclohexane-Et₃N). ¹H-NMR (300 MHz, (CD₃)₂CO) δ 8.17 (dd, 1H, $J_{7,8} = 8.4$ Hz, $J_{6,8} = 1.0$ Hz, H-8), 7.83 (d, 1H, $J_{5,6} = 8.3$ Hz, H-5), 7.56 (td, 1H, H-6), 7.42 (td, 1H, H-7), 3.27 (4H, m, 2 CH₂-N), 3.01 (t, 2H, $J_{H,H} = 6.5$ Hz, H-4), 2.96 (t, 2H, $J_{H,H} = 6.5$ Hz, H-1), 1.81 (m, 10H, 5CH₂) ppm. ¹³C-NMR (75.5 MHz, CD₃OD) δ 161.3 (C-4a), 156.5 (C-9), 148.5 (C-10a), 129.7, 128.5, 128.3, 127.3, 126.0, 125.5 (Ar-C), 53.2 (CH₂-N), 34.4 (C-4), 28.1 (C-1), 27.9, 25.7, 24.0, 23.7 (CH₂) ppm; HRESI-MS calcd. for C₁₈H₂₃N₂ ([M+H]⁺): 267.1856, found: 267.1854.

4.2.18. *N-[6'-(3'',4''-dihydroxybenzyl)amino]hexyl-1,2,3,4-tetrahydroacridin-9-amine (33)*. To a mixture of **31** (53.0 mg, 0.15 mmol) and 3,4-dibenzyloxybenzaldehyde (114.4 mg, 0.36 mmol, 2.4 equiv.) in toluene (2.5 mL) was added diethylamine (pH = 9-10). Then, it was refluxed under Ar for 6 h. Afterwards, it was concentrated to dryness, and the residue was dissolved in anhydrous MeOH (2.5 mL) and subjected to standard hydrogenolysis in the presence of Pd/C (75 mg) for 5 h. After that, the crude reaction mixture was filtered through a Celite® pad and concentrated to dryness. The residue

was purified by column chromatography ($\text{CH}_2\text{Cl}_2 \rightarrow 6:2:1 \text{ CH}_2\text{Cl}_2\text{-MeOH-AcOH}$). Yield: 19.6 mg, 30%; $R_f = 0.24$ (6:2:1:1 EtOAc-MeOH-AcOH-H₂O); $^1\text{H-NMR}$ (500 MHz, $(\text{CD}_3)_2\text{SO}$) δ 8.09 (d, 1H, $J_{7,8} = 8.5$ Hz, H-8), 7.69 (d, 1H, $J_{5,6} = 8.4$ Hz, H-5), 7.50 (brt, 1H, $J_{6,7} = 7.7$ Hz, H-6), 7.32 (brt, 1H, H-7), 6.74–6.50 (m, 3H, H-2'', H-5'', H-6''), 5.37 (s, 1H, NH), 3.56–3.38 (m, 4H, 2CH₂), 2.89 (brt, 2H, $J_{\text{H,H}} = 6.3$ Hz, H-4), 2.70 (brt, 2H, $J_{\text{H,H}} = 6.2$ Hz, H-1), 2.43 (s, 1H, NH), 1.81 (m, 6H, 3CH₂), 1.52 (m, 2H, CH₂), 1.36 (m, 2H, CH₂), 1.23 (m, 4H, 2CH₂) ppm; $^{13}\text{C-NMR}$ (125.7 MHz, $(\text{CD}_3)_2\text{SO}$) δ 172.8 (C-4a), 157.9 (C-1), 150.4 (C-10a), 146.9 (Ar-C), 145.2, 144.3 (C-3'', C-4''), 128.3, 127.9, 123.2, 123.0, 119.0 (Ar-C), 115.9 (C-9a), 115.8, 115.4 (C-2'', C-5''), 52.3, 48.0, 47.0 (N-CH₂, CH₂-CH₂N, Ar-CH₂), 33.6, 30.5, 29.0, 28.9, 26.6, 26.3, 22.8, 22.4 (CH₂) ppm; HRESI-MS calcd. for $\text{C}_{26}\text{H}_{34}\text{N}_3\text{O}_2$ ($[\text{M}+\text{H}]^+$): 420.2646, found: 420.2647.

4.2.19. *1-{2'-[(5''-Bromopentyl)oxy]ethyl}-4-methoxybenzene (38)*. To a solution of 2-(4-methoxyphenyl)ethanol (104.0 mg, 0.67 mmol) in anhydrous DMSO (4 mL) were added NaH (103.3 mg, 4.09 mmol, 6.1 equiv.) and 1,5-dibromopentane (753 μL , 5.36 mmol, 8.0 equiv.). The corresponding mixture was stirred at rt and under Ar for 5 h. After that, the solvent was removed *in vacuo*, and the residue was partitioned between 1:1 $\text{CH}_2\text{Cl}_2\text{-H}_2\text{O}$ (30 mL); the aqueous phase was extracted further with CH_2Cl_2 (2x15 mL). The combined organic fractions were dried over anhydrous Na_2SO_4 , filtrated and concentrated to dryness. The residue was purified by column chromatography (cyclohexane \rightarrow 1:15 Et₂O-cyclohexane 1:15). Yield: 114.8 mg, 57%; $R_f = 0.26$ (1:15 Et₂O-cyclohexane). $^1\text{H-NMR}$ (300 MHz, CDCl_3) δ 7.14 (m, 2H, H-2, H-6), 6.83 (m, 2H, H-3, H-5), 3.79 (s, 3H, OMe), 3.59 (t, 2H, $J_{\text{H,H}} = 7.0$ Hz, CH₂), 3.44 (t, 2H, $J_{\text{H,H}} = 7.0$ Hz, CH₂), 3.39 (t, 2H, $J_{\text{H,H}} = 7.0$ Hz, CH₂), 2.82 (t, 2H, $J_{\text{H,H}} = 7.0$ Hz, CH₂), 1.86 (quint., 2H, CH₂) 1.54 (m, 4H, 2CH₂) ppm; $^{13}\text{C-NMR}$ (75.5 MHz, CDCl_3) δ : 158.2 (C-4), 131.2 (C-1), 129.9 (C-2, C-6), 113.9 (C-3, C-5), 72.2 (Ar-CH₂-CH₂O), 70.7 (CH₂-O-CH₂), 55.4 (OMe), 35.6, 33.9, 32.7, 29.0, 25.1 (CH₂) ppm; HRESI-MS calcd. for $\text{C}_{14}\text{H}_{21}^{79}\text{BrNaO}_2$ ($[\text{M}+\text{Na}]^+$): 323.0617, found: 323.0617; calcd. for $\text{C}_{14}\text{H}_{21}^{81}\text{BrNaO}_2$ ($[\text{M}+\text{Na}]^+$): 325.0597, found 325.0595.

4.2.20. *4-{2'-[(5''-Bromopentyl)oxy]ethyl}-1,2-dimethoxybenzene (39)*. To a solution of 2-(3,4-dimethoxyphenyl)ethanol (102.5 mg, 0.55 mmol) in anhydrous DMSO (4 mL) were added NaH (84.5 mg, 3.4 mmol, 6.1 equiv.) and 1,5-dibromopentane (630 μL , 4.5

mmol, 8.2 equiv.). The resulting mixture was stirred at rt and under Ar for 4.5 hours. After that, it was partitioned between 1:1 Et₂O–H₂O (30 mL); the aqueous phase was extracted further with Et₂O (2x15 mL). The combined organic fractions were dried over Na₂SO₄, filtered and concentrated to dryness. The residue was purified by column chromatography (cyclohexane → 1:5 Et₂O–cyclohexane). Yield: 92.1 mg, 50%. *R*_f = 0.31 (1:2 Et₂O–cyclohexane). ¹H-NMR (300 MHz, CDCl₃) δ 6.77 (m, 3H, H-3, H-5, H-6), 3.86 (s, 3H, s, OMe), 3.85 (s, 3H, OMe), 3.60 (t, 2H, *J*_{H,H} = 7.1 Hz, CH₂), 3.44 (t, 2H, *J*_{H,H} = 7.1 Hz, CH₂), 3.39 (t, 2H, *J*_{H,H} = 7.1 Hz, CH₂), 2.82 (t, 2H, *J*_{H,H} = 7.1 Hz, CH₂), 1.86 (quint, 2H, CH₂), 1.64–1.43 (m, 4H, 2CH₂) ppm; ¹³C-NMR (75.5 MHz, CDCl₃) δ 148.9, 147.6 (C-1, C-2), 131.8 (C-4), 120.9 (C-5), 112.4, 111.3 (C-3, C-6), 72.2 (Ar-CH₂-CH₂), 70.8 (C-1''), 56.0 (OMe), 55.9 (OMe), 36.1, 33.9, 32.7, 29.0, 25.1 (CH₂) ppm; HRESI-MS calcd. for C₁₅H₂₃⁷⁹BrNaO₃ ([M+Na]⁺): 353.0723, found: 353.0721; calcd. for C₁₄H₂₁⁸¹BrNaO₂ ([M+Na]⁺): 355.0702, found 355.0700.

4.2.21. *1-Benzyloxy-4-[2'-{(5''-bromopentyl)oxy}ethyl]benzene (40)*. To a solution of 2-(4-(benzyloxy)phenyl)ethanol (100.1 mg, 0.44 mmol) in anhydrous DMF (5 mL) were added NaH (63.1 mg, 2.50 mmol, 5.7 equiv.) and 1,5-dibromopentane (480 μL, 3.42 mmol, 7.8 equiv.). The corresponding mixture was stirred at rt and under Ar for 5 h. After that, it was partitioned between 1:1 Et₂O–H₂O (30 mL); the aqueous phase was further extracted with Et₂O (2x15mL). The combined organic fractions were dried over Na₂SO₄, filtered and concentrated to dryness. The residue was purified by column chromatography (cyclohexane→1:10 Et₂O–cyclohexane). Yield: 103.6 mg, 63%; *R*_f= 0.82 (1:2 EtOAc–cyclohexane). ¹H-NMR (300 MHz, CDCl₃) δ 7.39 (m, 5H, m, Ar-H), 7.15 (m, 2H, H-3, H-5), 6.92 (m, 2H, H-2, H-6), 5.06 (s, 2H, Ph-CH₂), 3.60 (t, 2H, *J*_{H,H} = 7.1 Hz, CH₂), 3.45 (t, 2H, *J*_{H,H}= 6.4 Hz, CH₂), 3.40 (t, 2H, *J*_{H,H}= 6.8 Hz, CH₂), 2.84 (t, 2H, *J*_{H,H} = 7.1 Hz, CH₂), 1.87 (quint, 2H, CH₂), 1.60 (m, 2H, CH₂), 1.49 (m, 2H, CH₂) ppm; ¹³C-NMR (75.5 MHz, CDCl₃) δ 157.4 (C-1), 137.3 (C-1'), 131.5 (C-4), 130.0, 128.7, 128.0, 127.6 (Ar-C), 114.9 (C-2, C-6), 72.2 (C-2''), 70.7, 70.1 (Ph-CH₂O, C-1''), 35.6, 33.9, 32.7 (CH₂), 29.0 (C-2''), 25.1 (C-3'') ppm; HRESI-MS calcd. for C₂₀H₂₅⁷⁹BrNaO₂ ([M+Na]⁺): 399.0930, found: 399.0927.

4.2.22. *4-[2'-{(5''-Bromopentyl)oxy}ethyl]1,2-dibenzyloxybenzene (41)*. To a solution of 2-(3,4-dibenzyloxyphenyl)ethanol (41.7 mg, 0.12 mmol) in anhydrous DMSO (2

mL) were added NaH (20.5 mg, 0.81 mmol, 6.8 equiv.) and 1,5-dibromopentane (140 μ L, 1.0 mmol, 8.0 equiv.). The corresponding mixture was stirred at rt and under Ar for 5 h. After that, it was partitioned between 1:1 CH₂Cl₂–H₂O (30 mL); the aqueous layer was further extracted with CH₂Cl₂ (2x15 mL). The combined organic fractions were dried over Na₂SO₄, filtered and concentrated to dryness. The residue was purified by column chromatography (cyclohexane→1:15 Et₂O–cyclohexane). Yield: 40.7 mg, 70%; R_f = 0.39 (2:1 cyclohexane–Et₂O); ¹H-NMR (300 MHz, CDCl₃) δ 7.46 (m, 4H, Ar-H), 7.35 (m, 6H, Ar-H), 6.88 (d, 1H, $J_{5,6}$ = 8.2 Hz, H-6), 6.85 (d, 1H, $J_{3,5}$ = 2.0 Hz, H-3), 6.74 (dd, 1H, d, H-5), 5.15 (s, 2H, s, Ph-CH₂), 5.14 (s, 2H, Ph-CH₂), 3.56 (t, 2H, $J_{H,H}$ = 7.1 Hz CH₂), 3.42 (t, 2H, $J_{H,H}$ = 6.5 Hz, CH₂), 3.40 (t, 2H, $J_{H,H}$ = 6.8 Hz, CH₂), 2.79 (t, 2H, $J_{H,H}$ = 7.1 Hz CH₂) 1.86 (quint, 2H, $J_{H,H}$ = 7.1 Hz CH₂), 1.54 (m, 4H, 2CH₂) ppm; ¹³C-NMR (75.5 MHz, CDCl₃) δ 149.0, 147.6 (C-1, C-2), 137.6, 137.5 (Ar-C_{ipso}), 132.7 (C-4), 128.6 (Ar-C), 127.9 (Ar-C), 127.8 (Ar-C), 127.5 (Ar-C), 127.4 (Ar-C), 121.2 (Ar-C), 116.3, 115.4 (C-3, C-6), 72.0, 71.6, 71.5, 70.7 (CH₂-O), 36.0 (C-1'), 33.9, 32.7 (CH₂), 29.0 (C-2''), 25.0 (C-3'') ppm; HRESI-MS cacl. for C₂₇H₃₁⁷⁹BrNaO₃ ([M+Na]⁺): 505.1349, found: 505.1344; calcd. for C₂₇H₃₁⁸¹BrNaO₃ ([M+Na]⁺): 507.1328, found 507.1322.

4.2.23. N-[5'-(4''-Methoxyphenethyloxy)pentyl]-1,2,3,4-tetrahydroacridin-9-amine (**42**). To a solution of **38** (78.5 mg, 0.26 mmol) in anhydrous DMF (4.5 mL) were added tacrine (258.0 mg, 1.30 mmol, 5.0 equiv.) and KOH (430.7 mg, 6.5 mmol, 25.1 equiv.). The corresponding mixture was stirred at rt and under Ar for 4 h. After that, it was concentrated to dryness, and the residue was partitioned between 1:1 CH₂Cl₂–H₂O (30 mL); the aqueous layer was further extracted with CH₂Cl₂ (2x15 mL). The combined organic fractions were dried over Na₂SO₄, filtered and concentrated to dryness. The residue was purified by column chromatography (CH₂Cl₂→10:1 CH₂Cl₂–MeOH). Yield: 56.7 mg, 52%. R_f = 0.38 (10:5:1 EtOAc–cyclohexane–Et₃N). ¹H-NMR (300 MHz, CDCl₃) δ 8.03, 8.02 (2d, 1H each, $J_{H,H}$ = 9.0 Hz, $J_{H,H}$ = 9.1 Hz, H-5, H-8), 7.55 (1H, t, $J_{5,6}$ = $J_{6,7}$ = 7.6 Hz, H-6), 7.34 (t, 1H, $J_{7,8}$ = 7.6 Hz, H-7), 7.10 (m, 2H, H-2'', H-6''), 6.79 (m, 2H, H-3'', H-5''), 4.58 (s, 1H, NH), 3.73 (s, 3H, OMe), 3.56 (m, 4H, 2CH₂), 3.41 (t, 2H, $J_{H,H}$ = 6.1 Hz, CH₂), 3.10 (m, 2H, CH₂), 2.79 (t, 2H, $J_{H,H}$ = 7.1 Hz, CH₂), 2.66 (m, 2H, CH₂), 1.88 (m, 4H, 2CH₂), 1.74–1.36 (m, 6H, 3CH₂) ppm; ¹³C-

NMR (75.5 MHz, CDCl₃) δ 158.1, 156.6, 152.1, 145.3 (C-4a, C-9, C-10a, Ar-C-*p*), 131.1 (Ar-C), 129.8 (Ar-C-*o*), 129.4, 126.7, 124.0, 123.3, 119.1, 114.6 (Ar-C), 113.8 (Ar-C-*m*), 72.1, 70.6 (CH₂O), 55.3 (OMe), 49.2 (NH-CH₂), 35.5, 32.6, 31.4, 29.4, 24.6, 23.7, 22.8, 22.3 (CH₂) ppm; HRESI-MS calcd. for C₂₇H₃₅O₂N₂ ([M + H]⁺): 419.2693, found: 419.2684.

4.2.24. N-[5'-(3'',4''-Dimethoxyphenethyloxy)pentyl]-1,2,3,4-tetrahydroacridin-9-amine (**43**). To a solution of **39** (61.3 mg, 0.19 mmol) in anhydrous DMF (4 mL) were added tacrine (184.9 mg, 0.93 mmol, 5.0 equiv.) and KOH (309.8 mg, 4.7 mmol, 25.3 equiv.). The corresponding mixture was stirred at rt and under Ar for 4 h. After that, it was concentrated to dryness and partitioned between 1:1 CH₂Cl₂-H₂O (30 mL); the aqueous layer was further extracted with CH₂Cl₂ (2x15 mL). The combined organic fractions were dried over Na₂SO₄, filtered and concentrated to dryness. The residue was purified by column chromatography (CH₂Cl₂ → 20:1 CH₂Cl₂-MeOH). Yield: 20.7 mg, 25%. *R_f* = 0.19 (10:5:1 EtOAc-cyclohexane-Et₃N). ¹H-NMR (300 MHz, CDCl₃) δ 8.01, 7.96 (2m, H each, H-5, H-8), 7.57 (t, 1H, *J*_{5,6} = *J*_{6,7} = 7.4 Hz, H-6), 7.35 (t, 1H, *J*_{7,8} = 7.5 Hz, H-7), 6.75 (m, 3H, Ar-H), 4.17 (s, 1H, NH), 3.85 (s, 3H, OMe), 3.82 (s, 3H, OMe), 3.59 (t, 2H, *J*_{H,H} = 7.2 Hz, CH₂), 3.55 (t, 2H, *J*_{H,H} = 7.1 Hz, CH₂), 3.43 (t, 2H, *J*_{H,H} = 6.1 Hz, CH₂), 3.10 (m, 2H, CH₂), 2.81 (t, 2H, *J*_{H,H} = 6.9 Hz, CH₂), 2.67 (m, 2H, CH₂), 1.90 (m, 4H, 2CH₂), 1.74-1.36 (m, 6H, 3CH₂) ppm; ¹³C-NMR (75.5 MHz, CDCl₃) δ 157.3, 151.7, 148.9, 147.6 (C-4a, C-9, C-10a, C-3'', C-4''), 131.8, 129.1, 127.5, 124.0, 123.2, 120.9, 119.5, 115.1 (Ar-C), 112.4, 111.3 (C-2'', C-5''), 72.2, 70.7 (CH₂O), 56.0 (OMe), 55.9 (OMe), 49.4 (N-CH₂), 36.0, 31.6, 29.5, 24.7, 23.8, 23.0, 22.5 (CH₂) ppm; HRESI-MS calcd. for C₂₈H₃₇N₂O₃ ([M+H]⁺): 449.2799, found: 449.2789.

4.2.25. N-{5'-[4''-(Benzyloxyphenethyloxy)]pentyl}-1,2,3,4-tetrahydroacridin-9-amine (**44**). To a solution of **40** (94.2 mg, 0.25 mmol) in anhydrous DMF (4 mL) were added tacrine (251.5 mg, 1.27 mmol, 5.0 equiv.) and KOH (442.4 mg, 6.7 mmol, 26.8 equiv.). The corresponding mixture was stirred at rt for 5 h. Then, it was concentrated to dryness and partitioned between 1:1 CH₂Cl₂-H₂O (30 mL); the aqueous layer was further extracted with CH₂Cl₂ (2x15 mL). The combined organic fractions were dried over Na₂SO₄, filtered and concentrated to dryness. The residue was purified by column

chromatography (CH₂Cl₂ → 10:1 CH₂Cl₂-MeOH). Yield: 53.1 mg, 43%; *R_f* = 0.45 (10:5:1 EtOAc-cyclohexane-Et₃N). ¹H-NMR (300 MHz, CDCl₃) δ 7.97 (dd, 1H, *J*_{7,8} = 8.5 Hz, *J*_{6,8} = 0.8 Hz, H-8), 7.91 (dd, 1H, *J*_{5,6} = 8.5 Hz, *J*_{5,7} = 0.8 Hz, H-5), 7.54 (ddd, 1H, *J*_{6,7} = 8.2 Hz, H-6), 7.43–7.28 (m, 6H, Ar-H), 7.13 (m, 2H, Ar-H-*o*), 6.90 (m, 2H, Ar-H-*m*), 5.01 (s, 2H, Ph-CH₂), 3.93 (s, 1H, NH), 3.58 (t, 2H, *J*_{H,H} = 7.3 Hz, CH₂), 3.47 (t, 2H, *J*_{H,H} = 7.1 Hz, CH₂), 3.43 (t, 2H, *J*_{H,H} = 6.4 Hz, CH₂), 3.07 (m, 2H, CH₂), 2.82 (t, 2H, *J*_{H,H} = 7.1 Hz, CH₂), 2.71 (m, 2H, CH₂), 1.92 (m, 4H, 2CH₂), 1.64 (m, 4H, 2CH₂), 1.46 (m, 2H, CH₂) ppm; ¹³C-NMR (75.5 MHz, CDCl₃) δ 158.6, 157.5 (C-4a, C-4''), 150.7, 147.7 (C-9, C-10a), 137.2 (Ar-C_{ipso}), 131.4 (Ar-C-1''), 129.9 (C-2'', C-6''), 128.9 (Ar-C), 128.6 (Ar-C-*m*), 128.3, 128.0 (Ar-C), 127.5 (Ar-C-*o*), 123.7, 122.9, 120.4, 116.1 (Ar-C), 114.8 (C-3'', C-5''), 72.1, 70.7, 70.1 (CH₂O), 49.5 (N-CH₂), 35.5, 34.2, 31.6, 29.5, 24.9, 23.7, 23.2, 22.9 (CH₂) ppm; HRESI-MS calcd. for C₃₃H₂₉N₂O₂ ([M+H]⁺): 495.3006, found: 495.2998.

4.2.26. N-{5'-[3'',4''-(Dibenzyloxy)phenethyloxy]pentyl}-1,2,3,4-tetrahydroacridin-9-amine (**45**). To a solution of **41** (38.3 mg, 0.079 mmol) in anhydrous DMF (2 mL) were added tacrine (78.7 mg, 0.40 mmol, 5.0 equiv.) and KOH (131.2 mg, 1.99 mmol, 25.1 equiv.). The corresponding mixture was stirred at rt and under Ar for 4 h. Then, it was concentrated to dryness and partitioned between 1:1 CH₂Cl₂-H₂O (30 mL); the aqueous layer was further extracted with CH₂Cl₂ (2x15 mL). The combined organic fractions were dried over Na₂SO₄, filtered and concentrated to dryness. The residue was purified by column chromatography (CH₂Cl₂→ 10:1 CH₂Cl₂-MeOH). Yield: 31.5 mg, 66%; *R_f* = 0.45 (10:1 CH₂Cl₂-MeOH). ¹H-NMR (300 MHz, CDCl₃) δ 8.17 (d, 1H, *J*_{7,8} = 8.4 Hz, H-8), 7.99 (d, 1H, *J*_{5,6} = 8.1 Hz, H-5), 7.52 (td, 1H, *J*_{6,7} = 8.1 Hz, *J*_{6,8} = 1.0 Hz, H-6), 7.27 (m, 11H, Ar-H), 6.78 (d, 1H, *J*_{5'',6''} = 8.3 Hz, H-5''), 6.77 (d, 1H, *J*_{2'',6''} = 1.7 Hz, H-2''), 6.65 (dd, 1H, H-6''), 5.04, 5.01 (2s, 2H each, Ph-CH₂), 3.61 (t, 2H, t, *J*_{H,H} = 7.2 Hz, CH₂O), 3.48 (t, 2H, *J*_{H,H} = 7.2 Hz, CH₂), 3.34 (t, 2H, *J*_{H,H} = 6.1 Hz, CH₂), 3.09 (m, 2H, CH₂), 2.69 (t, 2H, *J*_{H,H} = 7.0 Hz, CH₂), 2.53 (m, 2H, CH₂), 1.78 (m, 4H, 2CH₂), 1.66 (quint, 2H, *J*_{H,H} = 7.4 Hz, CH₂), 1.52 (quint, 2H, *J*_{H,H} = 6.8 Hz, CH₂), 1.38 (m, 2H, CH₂) ppm; ¹³C-NMR (75.5 MHz, CDCl₃) δ 154.5, 153.5, 149.0, 149.7, 142.7 (C-4a, C-9, C-10a, C-3'', C-4''), 137.5, 137.4, 132.7, 130.6, 128.5, 127.9, 127.9, 127.5, 127.4, 124.5, 123.7, 122.0, 117.8, 116.4, 115.4, 113.1 (Ar-C), 72.0, 71.6, 70.6 (CH₂O), 49.0 (N-CH₂), 35.9, 31.2, 29.3, 24.2, 23.7, 22.5, 21.7 (CH₂) ppm; HRESI-MS calcd. for C₄₀H₄₅N₂O₃ ([M+H]⁺): 601.3425, found: 601.3415.

4.2.27. N-[5'-(4''-Hydroxyphenethyloxy)pentyl]-1,2,3,4-tetrahydroacridin-9-amine (**46**). A mixture of **44** (38.5 mg, 0.078 mmol) and 20% Pd(OH)₂ (20 mg) in CH₂Cl₂ (2 mL) was hydrogenated at rt and 1 atm for 1 h. After that, it was filtrated through a Celite® pad, and concentrated to dryness. The residue was purified by column chromatography (CH₂Cl₂→ 5:1 CH₂Cl₂-MeOH). Yield: 14.0 mg, 44%; R_f= 0.41 (15:5:2 EtOAc-cyclohexane-Et₃N). ¹H-NMR (300 MHz, CD₃OD) δ 8.24 (d, 1H, J_{7,8} = 8.4 Hz, H-8), 7.73 (m, 2H, H-5, H-6), 7.48 (m, 1H, H-7), 6.99 (m, 2H, H-2'', H-6''), 6.66 (m, 2H, H-3'', H-5''), 3.74 (t, 2H, J_{H,H} = 7.2 Hz, CH₂O), 3.54 (t, 2H, J_{H,H} = 6.9 Hz, CH₂), 3.42 (t, 2H, J_{H,H} = 6.1 Hz, CH₂), 2.98 (m, 2H, CH₂), 2.70 (m, 4H, 2CH₂), 1.93 (m, 4H, 2CH₂), 1.73 (m, 2H, CH₂), 1.56 (m, 2H, CH₂), 1.43 (m, 2H, CH₂) ppm; ¹³C-NMR (75.5 MHz, CD₃OD) δ 156.8, 155.8, 154.9, 143.3 (C-4a, C-9, C-10a, C-4''), 132.2, 131.1 (Ar-C), 130.8 (C-2'', C-6''), 125.6, 123.5, 118.9 (Ar-C), 116.0 (C-3'', C-5''), 114.6 (Ar-C), 73.2, 71.5 (CH₂O), 49.4 (N-CH₂), 36.3, 31.5, 31.4, 30.2, 25.4, 24.5, 23.5, 22.6 (CH₂) ppm; HRESI-MS calcd. for C₂₆H₃₃N₂O₂ ([M+H]⁺): 405.2537, found: 405.2526.

4.2.28. N-{5'-[3'',4''-(Dihydroxy)phenethyloxy]pentyl}-1,2,3,4-tetrahydroacridin-9-amine (**47**). A mixture of **45** (17.3 mg, 0.029 mmol) and 20% Pd(OH)₂ (10 mg) in CH₂Cl₂ (2 mL) was hydrogenated at rt and atm for 2.5 h. After that, it was filtered through a Celite® pad and concentrated to dryness. The residue was purified by column chromatography (CH₂Cl₂→ 5:1 CH₂Cl₂-MeOH). Yield: 7.3 mg, 60%; R_f = 0.21 (15:5:2 EtOAc-cyclohexane-Et₃N). ¹H-NMR (500 MHz, CD₃OD) δ 8.34 (d, 1H, J_{7,8} = 8.5 Hz, H-8), 7.80 (m, 2H, H-5, H-6), 7.53 (brtd, 1H, J_{6,7} = J_{7,8} = 8.3 Hz, J_{5,7} = 0.9 Hz, H-7), 6.63 (d, 1H, J_{5'',6''} = 7.9 Hz, H-5''), 6.63 (d, 1H, J_{2'',6''} = 2.7 Hz, H-2''), 6.49 (dd, 1H, H-6''), 3.87 (t, 2H, J_{H,H} = 6.8 Hz, CH₂O), 3.58 (t, 2H, J_{H,H} = 6.8 Hz, CH₂), 3.46 (t, 2H, J_{H,H} = 6.1 Hz, CH₂), 3.02 (m, 2H, CH₂), 2.73 (m, 2H, CH₂), 2.68 (t, 2H, J_{H,H} = 7.1 Hz, CH₂), 1.94 (m, 4H, 2CH₂), 1.77 (quin, 2H, J_{H,H} = 7.4 Hz, CH₂), 1.56 (quint, 2H, J_{H,H} = 6.7 Hz, CH₂), 1.45 (m, 2H, CH₂) ppm; ¹³C-NMR (125.8 MHz, CD₃OD) δ 157.0, 153.3, 146.1, 144.6, 141.6 (C-4a, C9, C-10a, C-3'', C-4''), 133.1, 131.9, 126.1, 126.0, 121.8, 121.1, 118.0 (Ar-C), 117.0, 116.2 (C-2'', C-5''), 113.7 (Ar-C), 73.2, 71.5 (CH₂O), 36.6, 31.3, 30.7, 30.4, 30.1, 25.1, 24.5, 23.2, 22.2 (CH₂) ppm; HRESI-MS calcd. for C₂₆H₃₃N₂O₃ ([M+H]⁺): 421.2486, found: 421.2476.

Acknowledgements

We thank the Dirección General de Investigación of Spain (CTQ2016-78703-P), Junta de Andalucía (FQM134), FEDER (501100008530), the Italian Ministry of Education, Universities and Research (MIUR) and the University of Bologna for financial support. JMR-P thanks Spanish Ministerio de Educación for the award of a fellowship. COST Action *Multi-target paradigm for innovative ligand identification in the drug discovery process (MuTaLig)* (CA15135) is also acknowledged. We would also like to thank the Servicio de Resonancia Magnética Nuclear, CITIUS (University of Seville) for the performance of NMR experiments.

References

-
- [1] A. Alzheimer, Über einen eigenartigen schweren Erkrankungsprozeß der Hirnrinde, *Neurologisches Centralblatt* 23 (1906) 1129–1136.
 - [2] D.M. Holtzman, J.C. Morris, A.M. Goate, Alzheimer's disease: the challenge of the second century, *Sci Transl Med.* 3 (2011) 3:77sr1, <https://doi.org/10.1126/scitranslmed.3002369>.
 - [3] <https://www.alz.co.uk/research/world-report-2018>, last accessed 29th December 2018.
 - [4] <https://www.alz.co.uk/research/statistics>, last accessed 29th December 2018.
 - [5] F. Bature, B.-a. Guinn, D. Pang, Y. Pappas, Signs and symptoms preceding the diagnosis of Alzheimer's disease: a systematic scoping review of literature from 1937 to 2016, *BMJ Open* 7 (2017) e015746, <http://dx.doi.org/10.1136/bmjopen-2016-015746>.
 - [6] A. Kumar, A. Singh, Ekavali, A review on Alzheimer's disease pathophysiology and its management: an update, *Pharmacol Rep.* 67 (2015) 195–203.
 - [7] C. Reitz, R. Mayeux, Alzheimer disease: epidemiology, diagnostic criteria, risk factors and biomarkers, *Biochem. Pharmacol.* 88 (2014) 640–651.
 - [8] J. Wang, B.J. Gu, C.L. Masters, Y.J. Wang, A systemic view of Alzheimer disease - insights from amyloid- β metabolism beyond the brain, *Nat. Rev. Neurol.* 13 (2017) 612–623.
 - [9] L. Alves, A.S. Correia, R. Miguel, P. Alegria, P. Bugalho, Alzheimer's disease: a clinical practice-oriented review, *Front. Neurol.* 3 (2012) 63, <https://doi.org/10.3389/fneur.2012.00063>.
 - [10] B. Shal, W. Ding, H. Ali, Y. Kim, S. Khan, Anti-neuroinflammatory potential of natural products in attenuation of Alzheimer's disease, *Front. Pharmacol.* 9 (2018) 548, <https://doi.org/10.3389/fphar.2018.00548>.
 - [11] K.J. Barnham, A. Bush, Biological metals and metal-targeting compounds in major neurodegenerative diseases, *Chem. Soc. Rev.* 43 (2014) 6727–6749.
 - [12] J. Godyń, J. Jończyk, D. Panek, B. Malawska, Therapeutic strategies for Alzheimer's disease in clinical trials, *Pharmacol. Rep.* 68 (2016) 127–138.

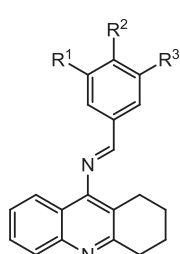
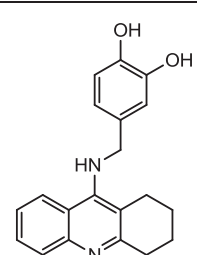
-
- [13] E. Simoni, M. Bartolini, I.F. Abu, A. Blockley, C. Gotti, G. Bottegoni, R. Caporaso, C. Bergamini, V. Andrisano, A. Cavalli, I.R. Mellor, A. Minarini, M. Rosini, Multitarget drug design strategy in Alzheimer's disease: focus on cholinergic transmission and amyloid- β aggregation, *Future Med. Chem.* 9 (2017) 953–963.
- [14] M.L. Bolognesi, E. Simoni, M. Rosini, A. Minarini, V. Tumiatti, C. Melchiorre, Multitarget-directed ligands: innovative chemical probes and therapeutic tools against Alzheimer's disease, *Curr. Top. Med. Chem.* 11 (2011) 2797–2806.
- [15] A. Cavalli, M.L. Bolognesi, A. Minarini, M. Rosini, V. Tumiatti, M. Recanatini, C. Melchiorre, Multi-target-directed ligands to combat neurodegenerative diseases, *J. Med. Chem.*, 51 (2008) 347–372.
- [16] S. M. Park, S.H. Ki, N.R. Han, I.J. Cho, S.K. Ku, S.C. Kim, R.J. Zhao, Y.W. Kim, Tacrine, an oral acetylcholinesterase inhibitor, induced hepatic oxidative damage, which was blocked by liquiritigenin through GSK3-beta inhibition, *Biol. Pharm. Bull.* 38 (2015) 184–192.
- [17] M. Girek, P. Szymański, Tacrine hybrids as multi- target- directed ligands in Alzheimer's disease: influence of chemical structures on biological activities, *Chem. Pap.* 2018, <https://doi.org/10.1007/s11696-018-0590-8>.
- [18] W. Osman, T. Mohamed, V.M. Sit, M.S. Vasefi, M.A. Beazely, P.P.N. Rao, Structure–activity relationship studies of benzyl-, phenethyl-, and pyridyl- substituted tetrahydroacridin- 9- amines as multitargeting agents to treat Alzheimer's disease, *Chem. Biol. Drug Des.* 88 (2016) 710–723.
- [19] R.E. Amariglio, M.C. Donohue, G.A. Marshall, D.M. Rentz, D.P. Salmon, S.H. Ferris, S. Karantzoulis, P.S. Aisen, R.A. Sperling, Alzheimer's Disease Cooperative Study, Tracking early decline in cognitive function in older individuals at risk for Alzheimer's disease dementia: the Alzheimer's Disease Cooperative Study Cognitive Function Instrument, *JAMA Neurol.* 72 (2015) 446–454.
- [20] A. Contestabile, The history of the cholinergic hypothesis, *Behav. Brain Res.* 221 (2011) 334–340.
- [21] N.H. Greig, D. Lahiri, K. Sambamurti, Butyrylcholinesterase: an important new target in Alzheimer's disease therapy, *Int. Psychogeriatr* 14 (2002) 77–91.
- [22] K. Lodarski, J. Jończyk, N. Guziar, M. Bajda, J. Gładysz, J. Walczyk, M. Jeleń, B. Morak-Młodawska, K. Pluta, B. Malawska, Discovery of butyrylcholinesterase inhibitors among derivatives of azaphenothiazines, *J. Enzyme Inhib. Med. Chem.* 30 (2015) 98–106.
- [23] I.R. Macdonalda, S.P. Maxwella, G.A. Reida, M.K. Casha, D.R. DeBaya, S. Darvesh, Quantification of butyrylcholinesterase activity as a sensitive and specific biomarker of Alzheimer's disease, *J. Alzheimers Dis.* 58 (2017) 491–505.
- [24] S.N. Dighe, G.S. Deora, E. De la Mora, F. Nachon, S. Chan, M.-O. Parat, X. Brazzolotto, B.P. Ross, Discovery and structure–activity relationships of a highly selective butyrylcholinesterase inhibitor by structure-based virtual screening, *J. Med. Chem.* 59 (2016) 7683–7689.
- [25] G.L. Ellman, K.D. Courtney, V. Andres Jr., R.M. Featherstone, A new and rapid colorimetric determination of acetylcholinesterase activity, *Biochem. Pharmacol.* 7 (1961) 88–95.

-
- [26] J.M. Roldán-Peña, D. Alejandre-Ramos, Ó. López, I. Maya, I. Lagunes, J.M. Padrón, L.E. Peña-Altamira, M. Bartolini, B. Monti, M.L. Bolognesi, J.G. Fernández-Bolaños, New tacrine dimers with antioxidant linkers as dual drugs: anti-Alzheimer's and antiproliferative agents, *Eur. J. Med. Chem.* 138 (2017) 761–773.
- [27] W. Luo, Y.-P. Li, Y. He, S.-L. Huang, D. Li, L.-Q. Gu, Z.-S. Huan, Synthesis and evaluation of heterobivalent tacrine derivatives as potential multi-functional anti-Alzheimer agents, *Eur. J. Med. Chem.* 46 (2011) 2609–2616.
- [28] A. McEneny-King, W. Osman, A.N. Edginton, P.P.N. Rao, Cytochrome P450 binding studies of novel tacrine derivatives: predicting the risk of hepatotoxicity, *Bioorg. Med. Chem. Lett.* 27 (2017) 2443–2449.
- [29] A. Saxena, A.M.G. Redman, X. Jiang, O. Lockridge, B.P. Doctor, Differences in active site gorge dimensions of cholinesterases revealed by binding of inhibitors to human butyrylcholinesterase, *Biochemistry* 36 (1997) 36 14642–14651.
- [30] H. Naiki, K. Higuchi, K. Nakakuki, T. Takeda, Kinetic analysis of amyloid fibril polymerization in vitro, *Lab. Invest* 65 (1991) 104–110.
- [31] M.L. Bolognesi, M. Bartolini, F. Mancini, G. Chiriano, L. Ceccarini, M. Rosini, A. Milelli, V. Tumiatti, V. Andrisano, C. Melchiorre, Bis(7)-tacrine derivatives as multitarget-directed ligands: focus on anticholinesterase and anti-amyloid activities, *ChemMedChem* 5 (2010) 1215–1220.
- [32] N. Nardi, G. Avidan, D. Daily, R. Zilkha-Falb, A. Barzilai, Biochemical and temporal analysis of events associated with apoptosis induced by lowering the extracellular potassium concentration in mouse cerebellar granule neurons, *J. Neurochem.* 68 (1997) 750–759.
- [33] L. Huang, J. Lin, S. Xiang, K. Zhao, J. Yu, J. Zheng, D. Xu, S. Mak, S. Hu, S. Nirasha, C. Wang, X. Chen, J. Zhang, S. Xu, X. Wei, Z. Zhang, D. Zhou, W. Zhou, W. Cui, Y. Han, Z. Hu, Q. Wang, Sunitinib, a clinically used anticancer drug, is a potent AChE inhibitor and attenuates cognitive impairments in mice, *ACS Chem. Neurosci.* 7 (2016) 1047–1056.
- [34] F. Nachon, E. Carletti, C. Ronco, M. Trovaslet, Y. Nicolet, L. Jean, P.-Y. Renard, Crystal structures of human cholinesterases in complex with huprine W and tacrine: elements of specificity for anti-Alzheimer's drugs targeting acetyl- and butyryl-cholinesterase, *Biochem. J.* 453 (2013) 393–399.
- [35] Maestro, version 9.1, Schrödinger, LLC, New York, NY, 2010.
- [36] A. Pesaresi, S. Samez, D. Lamba, 4W63: Torpedo californica acetylcholinesterase in complex with a tacrine-benzofuran hybrid inhibitor, [10.2210/pdb4W63/pdb](https://doi.org/10.2210/pdb4W63/pdb).
- [37] M. J. Frisch, G. W. Trucks, H. B. Schlegel, G. E. Scuseria, M. A. Robb, J. R. Cheeseman, G. Scalmani, V. Barone, B. Mennucci, G. A. Petersson, H. Nakatsuji, M. Caricato, X. Li, H. P. Hratchian, A. F. Izmaylov, J. Bloino, G. Zheng, J. L. Sonnenberg, M. Hada, M. Ehara, K. Toyota, R. Fukuda, J. Hasegawa, M. Ishida, T. Nakajima, Y. Honda, O. Kitao, H. Nakai, T. Vreven, J. A. Montgomery, Jr., J. E. Peralta, F. Ogliaro, M. Bearpark, J. J. Heyd, E. Brothers, K. N. Kudin, V. N. Staroverov, R. Kobayashi, J. Normand, K. Raghavachari, A. Rendell, J. C. Burant, S. S. Iyengar, J. Tomasi, M. Cossi, N. Rega, J. M. Millam, M. Klene, J. E. Knox, J. B. Cross, V. Bakken, C. Adamo, J. Jaramillo, R. Gomperts, R. E. Stratmann, O. Yazyev, A. J. Austin, R. Cammi, C. Pomelli, J. W. Ochterski, R. L. Martin, K. Morokuma, V. G. Zakrzewski, G. A. Voth, P. Salvador, J. J.

-
- Dannenberg, S. Dapprich, A. D. Daniels, Ö. Farkas, J. B. Foresman, J. V. Ortiz, J. Cioslowski and D. J. Fox, Gaussian 09 C.01, Gaussian, Inc., Wallingford, CT, 2009.
- [38] S. Grimme, J. Antony, S. Ehrlich, H. Krieg, A consistent and accurate ab initio parametrization of density functional dispersion correction (DFT-D) for the 94 elements H-Pu, *J. Chem. Phys.* 132 (2010) 154104, <https://doi.org/10.1063/1.3382344>.
- [39] S. F. Boys, F. Bernardi, The calculation of small molecular interactions by the differences of separate total energies. Some procedures with reduced errors. *Mol. Phys.* 19 (1970) 553–566.
- [40] E. Uliassi, L.E. Peña-Altamira, A.V. Morales, F. Massenzio, S. Petralla, M. Rossi, M. Roberti, L. Martínez González, A. Martínez, B. Monti, M.L. Bolognesi, A focused library of psychotropic analogues with neuroprotective and neuroregenerative potential, *ACS Chem. Neurosci.*, *In Press*, <https://doi.org/10.1021/acchemneuro.8b00242>
- [41] P.O. Miranda, J.M. Padron, J.I. Padron, J. Villar, V.S. Martín, Prins-type synthesis and SAR study of cytotoxic alkyl chloro dihydropyrans, *ChemMedChem* 1 (2006) 323–329.

Table 1. Inhibitory properties of tacrine-polyphenols ($K_i \pm SD$)							
Compound	Series	AChE (<i>electric eel</i>)		Type of inhibitor	BuChE (equine serum)		Type of inhibitor
		K_{ia} (μM)	K_{ib} (μM)		K_{ia} (nM)	K_{ib} (nM)	
6	Imine	2.5 ± 0.6	1.9 ± 0.4	Mixed	271 ± 36	35 ± 8	Mixed
7		39 ± 10	23 ± 6		2925 ± 1183	643 ± 327	
8		24 ± 4	20 ± 1		637 ± 79	173 ± 42	
9		2.3 ± 0.8	3.0 ± 0.8		704 ± 82	192 ± 74	
10	Amine (1C)	0.64 ± 0.08	0.21 ± 0.06		31 ± 6	6.4 ± 1.3	Uncompetitive
11	Imine	3.0 ± 0.6	1.8 ± 0.1		---	17 ± 5	
12	Amine (1C)	0.37 ± 0.04	0.081 ± 0.013		12 ± 2	3.2 ± 0.5	
13	Imine	2.1 ± 0.3	0.82 ± 0.27		11 ± 4	1.9 ± 0.8	
14	Amine (1C)	0.19 ± 0.06	0.19 ± 0.06		Non-competitive	25 ± 6	3.2 ± 1.2
15	Imine	0.40 ± 0.19	0.17 ± 0.04		Mixed	51 ± 17	5.8 ± 1.5
19	Amine (2C)	1.6 ± 0.5	0.61 ± 0.15	Mixed	22 ± 7	1.1 ± 0.6	
20a		0.11 ± 0.01	0.032 ± 0.005	Mixed	184 ± 46 (Uncompetitive)		
20b		0.87 ± 0.43	0.59 ± 0.38	Mixed	128 ± 20	28 ± 9	
25	Cyclic amine	3.2 ± 0.8	---	Competitive	1202 ± 130	304 ± 81	
27		1.8 ± 1.2	2.5 ± 1.5	Mixed	1898 ± 590	275 ± 105	
32	Amine (5- and 6C)	0.16 ± 0.09	0.12 ± 0.03		30 ± 14	9.9 ± 3.7	
33	0.12 ± 0.05	0.058 ± 0.015	7.9 ± 1.0		1.7 ± 0.4		
42	Ether	0.075 ± 0.028	0.075 ± 0.028		Non-competitive	29 ± 5	2.9 ± 1.1

43		0.17 ± 0.02	0.055 ± 0.016	Mixed	7.0 ± 0.4	1.9 ± 0.8	
44		0.11 ± 0.02	0.11 ± 0.02	Non-competitive	1.9 ± 0.9	1.5 ± 0.9	
45		0.34 ± 0.05	0.13 ± 0.03	Mixed	4.6 ± 0.6	2.7 ± 0.9	
46		0.14 ± 0.02	0.10 ± 0.06		---	4.5 ± 1.5	Uncompetitive
47		0.21 ± 0.02	0.077 ± 0.016		43 ± 7	9.0 ± 2.2	Mixed
Tacrine		0.023 ± 0.010	---	Competitive	17 ± 3	---	Competitive
Galantamine		3.0 ± 0.9	---		7700 ± 1700	---	

Compound		hAChE (IC ₅₀ , nM)	hBuChE (IC ₅₀ , nM)	Selectivity index (SI)	%Inhibition Aβ ₄₂ self-aggregation (at 50 μM)
11		1475 ± 311	194 ± 15	7.6	---
13		609 ± 26	41.5 ± 4.06	14.8	---
15		1040 ± 40	120 ± 49	8.7	---
14		100 ± 13	74.8 ± 3.4	1.3	---

---		25.6 ± 0.9 Ref [Error! Bookmark not defined.]	7.50 ± 0.02 Ref [Error! Bookmark not defined.]	3.4	---
33		29.0 ± 1.3	22.9 ± 1.2	1.3	---
42 (R ¹ = H, R ² = OMe)		216 ± 45	2.92 ± 0.26	74.5	63.5 ± 1.0
43 (R ¹ = R ² = OMe)		168 ± 37	0.515 ± 0.050	323.1	63.8 ± 4.8
44 (R ¹ = H, R ² = OBn)		454 ± 69	6.95 ± 0.21	65.8	70.0 ± 4.8
45 (R ¹ = R ² = OBn)		506 ± 64	0.497 ± 0.059	1012	75.3 ± 0.4
46 (R ¹ = H, R ² = OH)		142 ± 16	6.06 ± 0.59	23.3	54.4 ± 6.6
47 (R ¹ = R ² = OH)		542 ± 16	35.6 ± 2.1	15.2	(*)
Tacrine			412 ± 15	44.2 ± 1.7	9.3
Bis(7)tacrine		0.81 ± 0.09 [Error! Bookmark not defined.]	---	---	71.1 ± 0.7 [Error! Bookmark not defined.]

(*) Not tested, due to significant interference (quenching of the Thioflavin T fluorescence signal)

Figure 1
[Click here to download high resolution image](#)

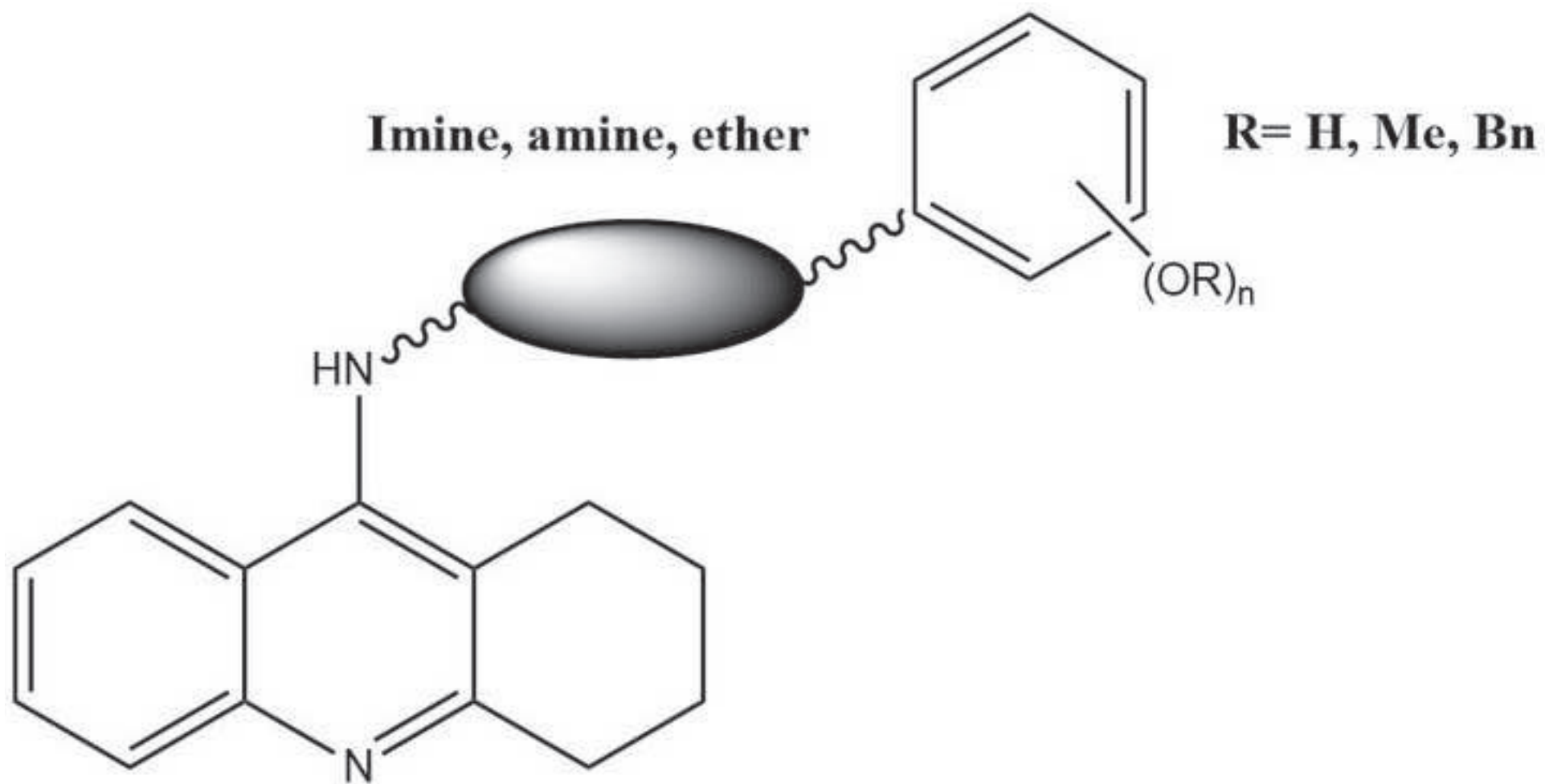


Figure 2
[Click here to download high resolution image](#)

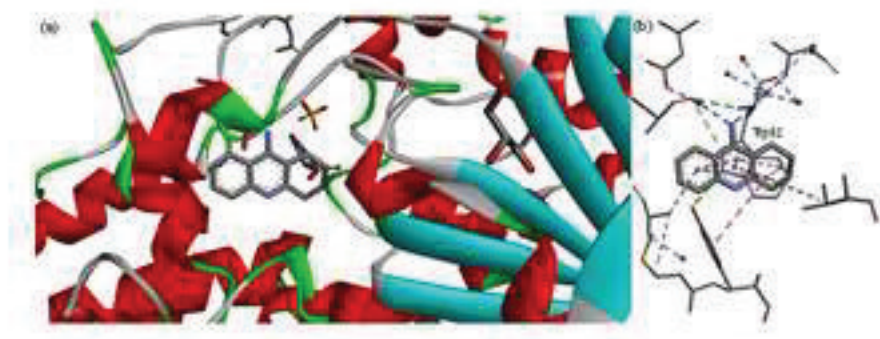


Figure 3
[Click here to download high resolution image](#)

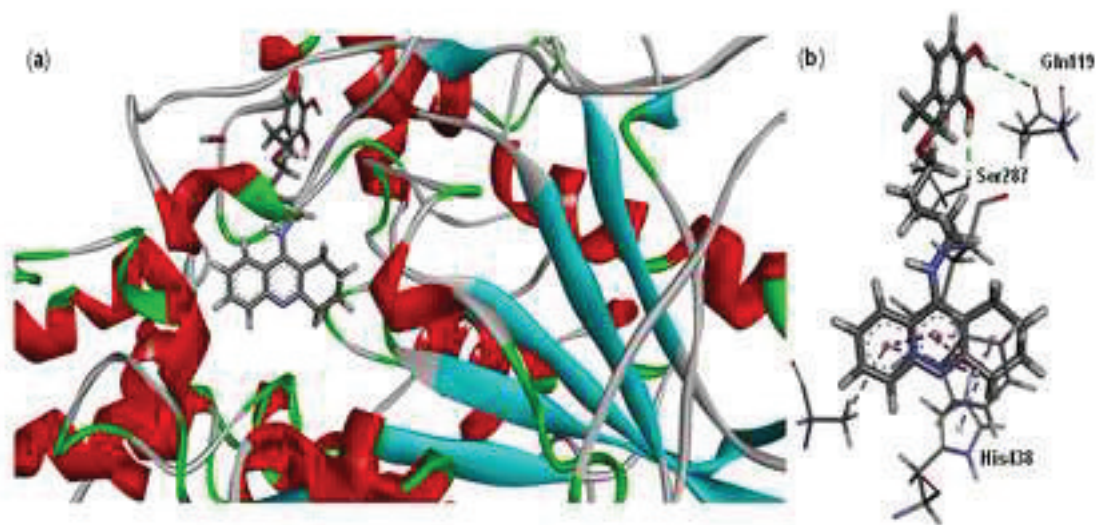


Figure 4
[Click here to download high resolution image](#)

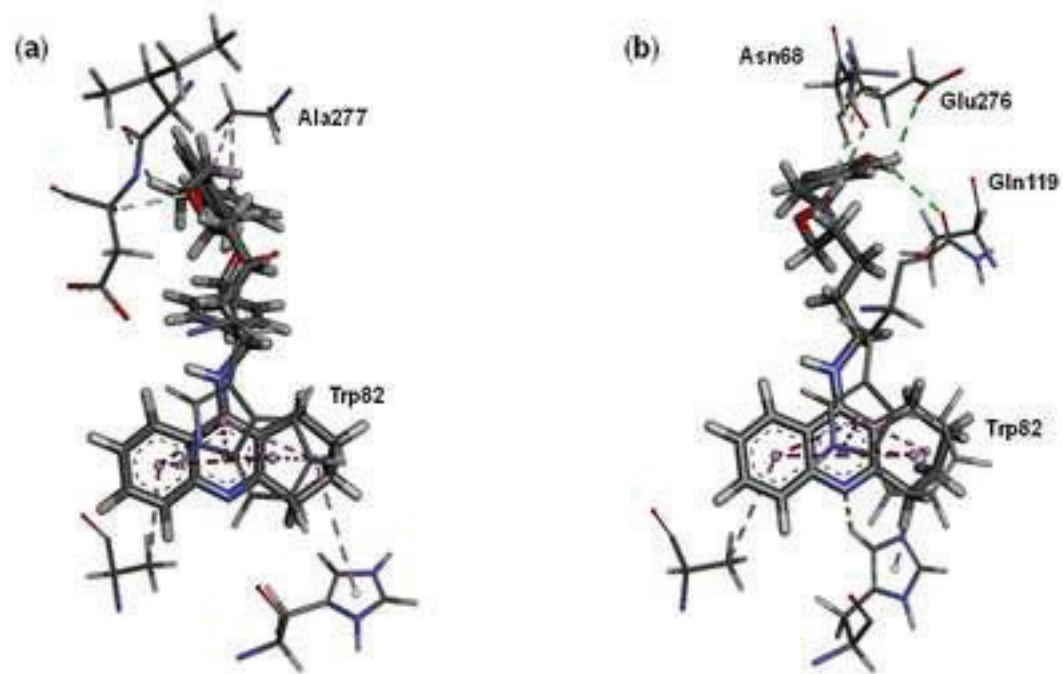


Figure 5
[Click here to download high resolution image](#)

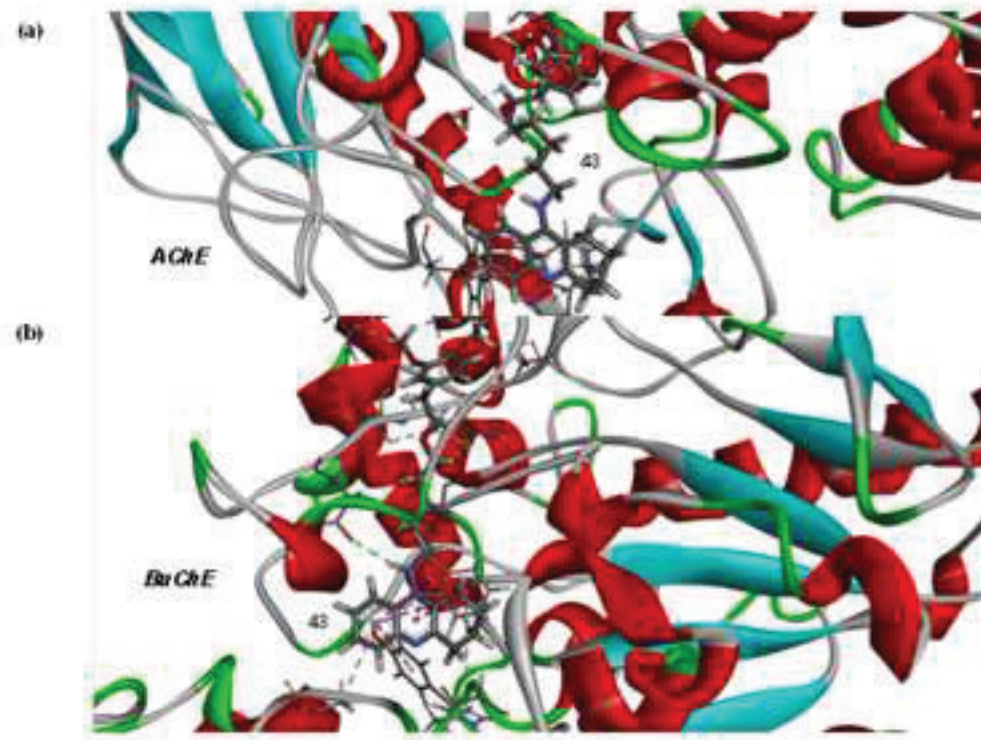
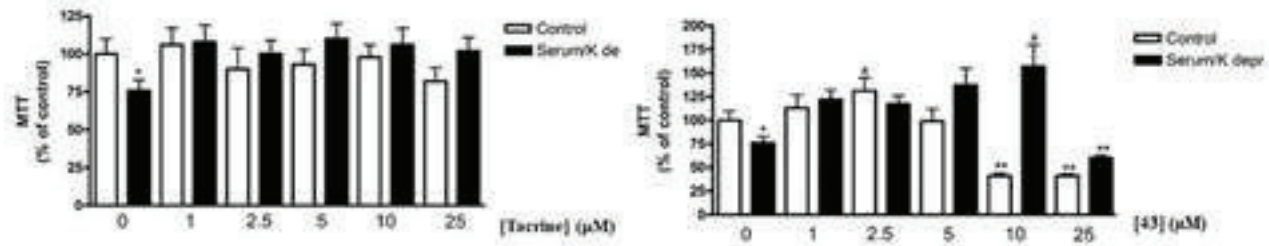
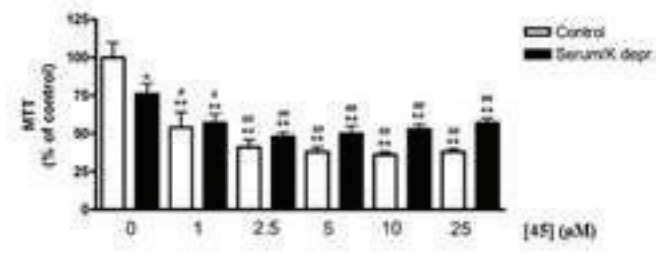


Figure 6
[Click here to download high resolution image](#)



(A)

(B)



(C)

Figure 7
[Click here to download high resolution image](#)

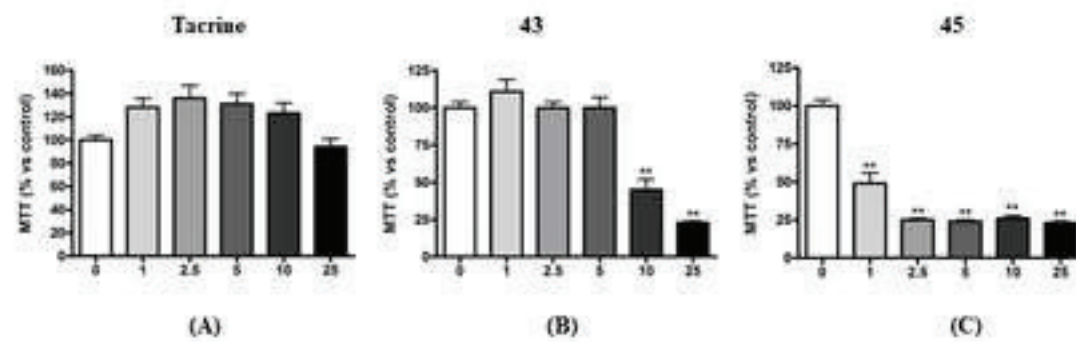


Figure 8
[Click here to download high resolution image](#)

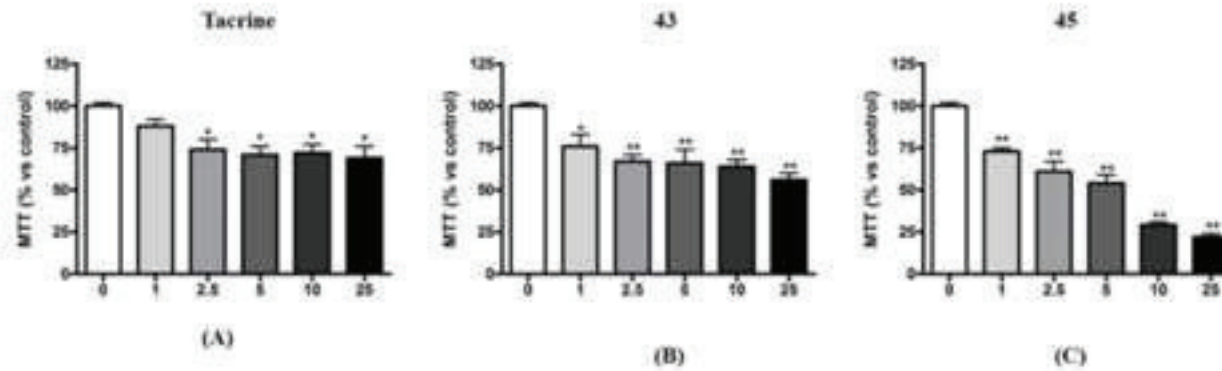
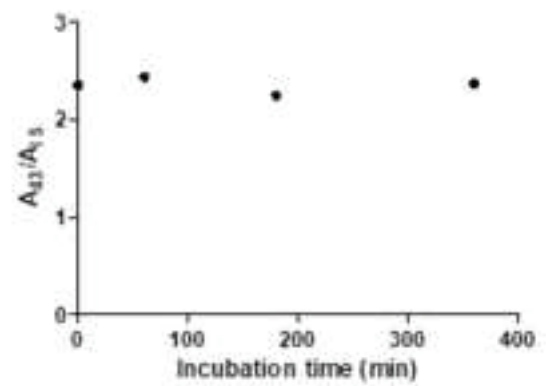
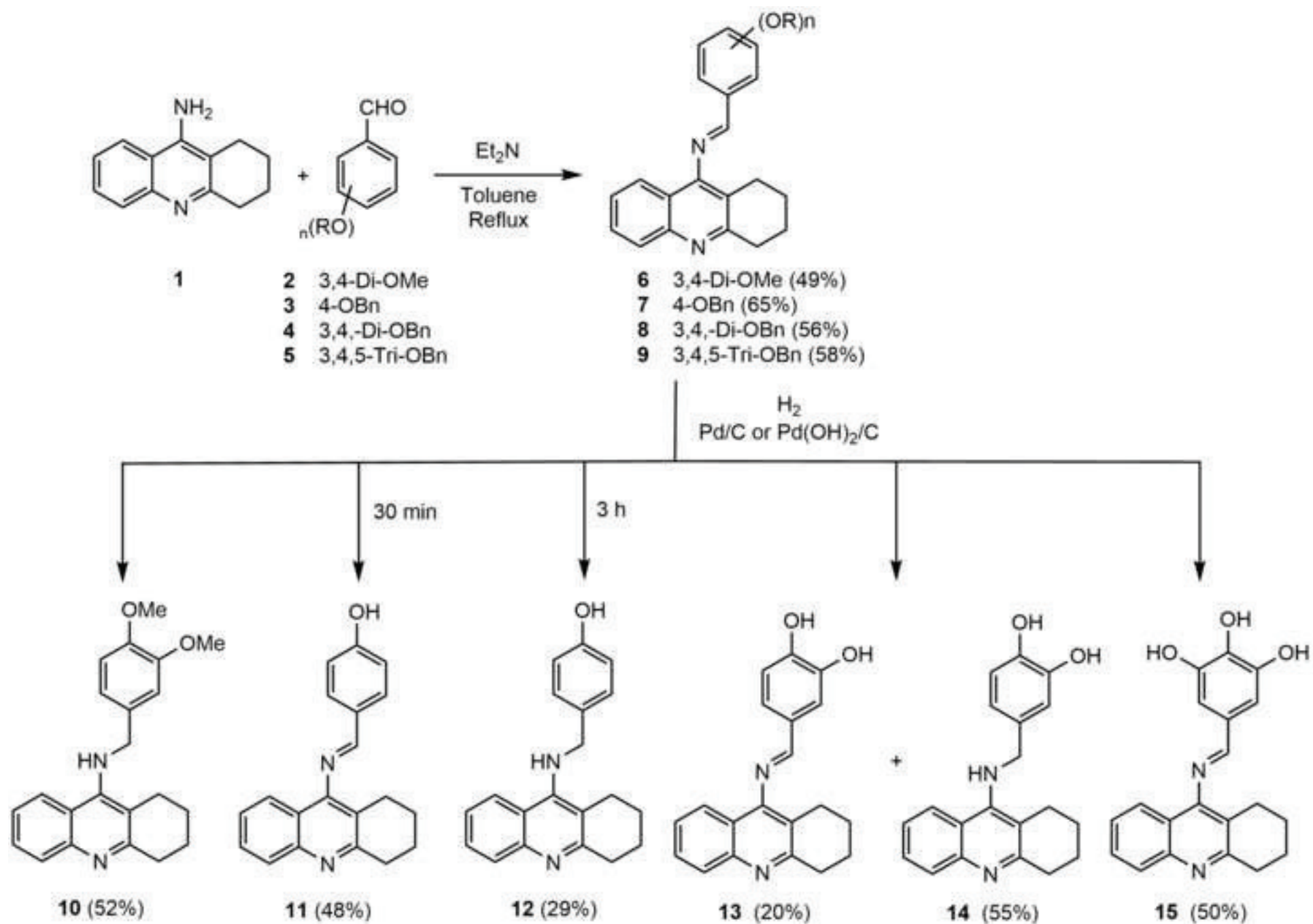


Figure 9
[Click here to download high resolution image](#)

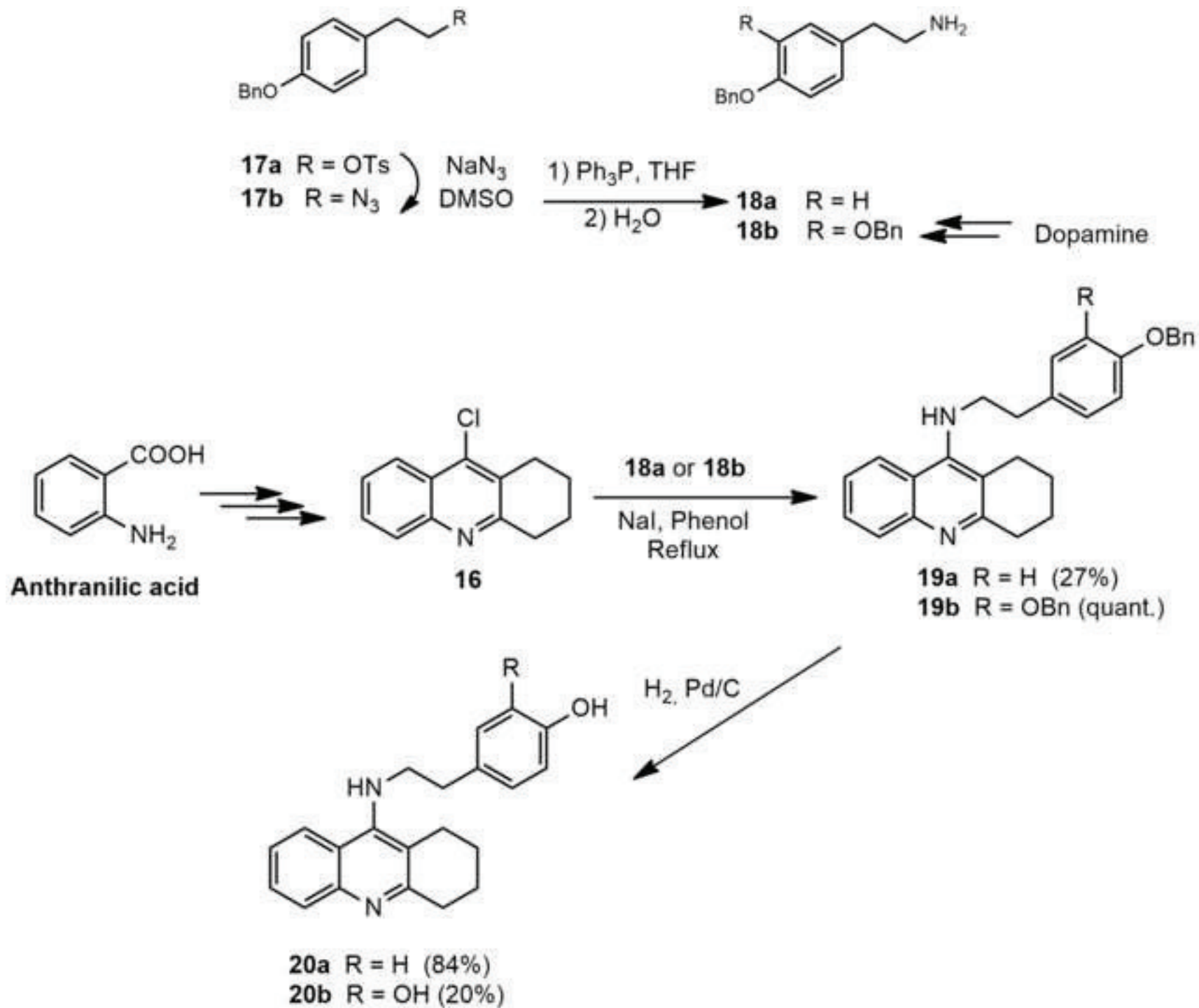


Scheme 1

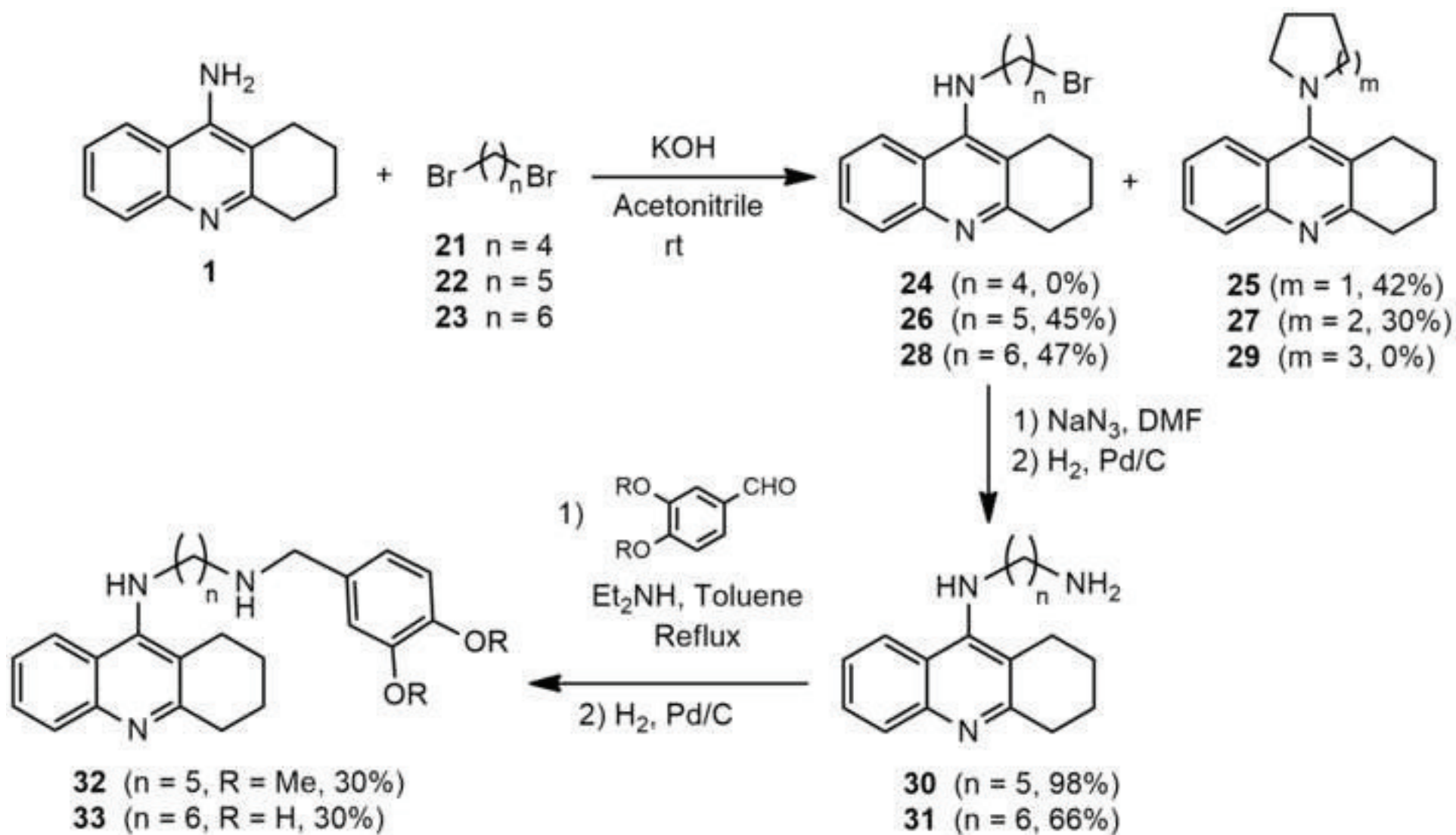
[Click here to download high resolution image](#)



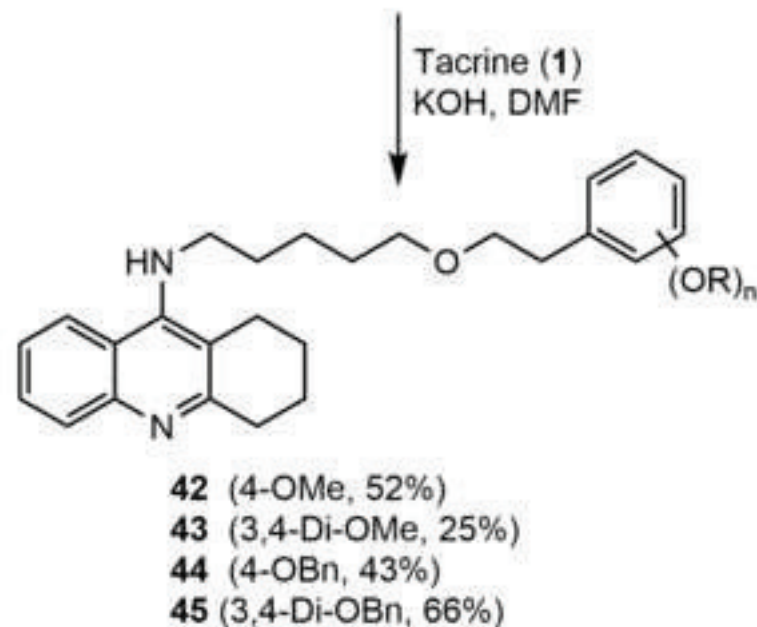
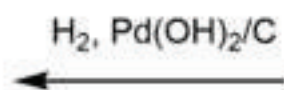
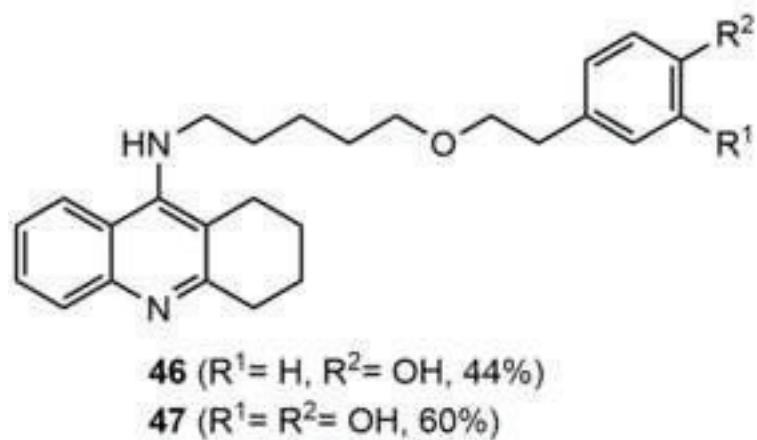
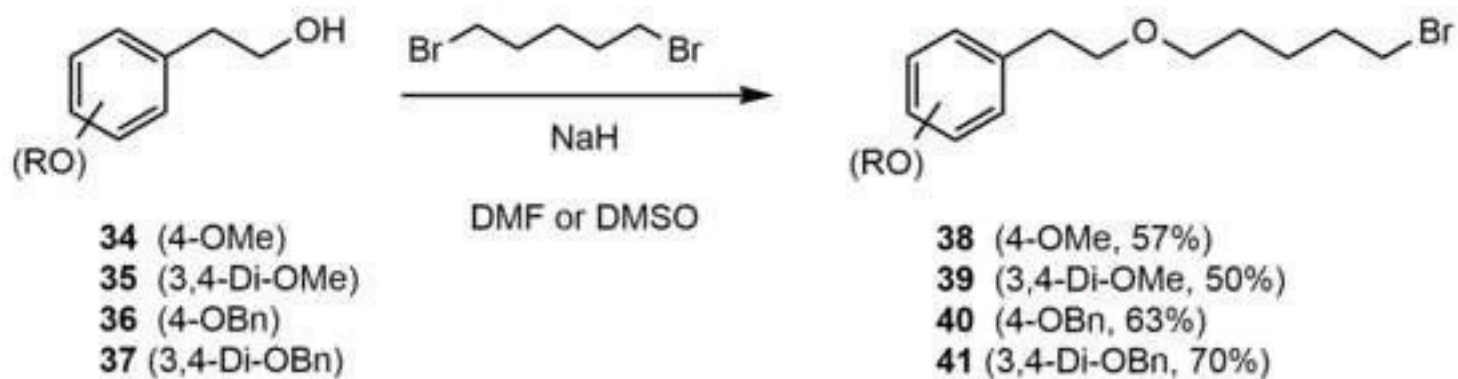
Scheme 2

[Click here to download high resolution image](#)

Scheme 3

[Click here to download high resolution image](#)

Scheme 4

[Click here to download high resolution image](#)

Supplementary Material

[Click here to download Supplementary Material - For Review Purposes Only: Supporting Information - revised.docx](#)